SARCO(ENDO)PLASMIC RETICULUM CALCIUM ATPASE AND PHOSPHOLAMBAN REMODELLING IN AN OVINE MYOCARDIAL INFARCTION MODEL

A thesis submitted to The University of Manchester for the degree of Master of Philosophy in the Faculty of Biology, Medicine and Health

2022

Yilan Shen

Division of Cardiovascular Sciences

List of Contents

Word counts: 21220

Abbreviation

CAMKII	Ca^{2+}/calmodulin-dependent protein kinase II
cAMP	Cyclic adenosine monophosphate
CICR	Calcium induced calcium release
CRU	Calcium release unit
ECC	Excitation-contraction coupling
HFmrEF	Heart failure with mid-range ejection fraction
HFpEF	Heart failure with preserved ejection fraction
HFrEF	Heart failure with reduced ejection fraction
ISO	Isoprenaline
LTCC	L-type calcium channel
NCX	Na^{+}-Ca^{2+} exchanger
PKA	Protein kinase A
PLN	Phospholamban
PP1	Protein phosphatase 1
RIPA	Radioimmunoprecipitation assay
RyRs	Ryanodine receptors
SAN	Sinoatrial node
Ser16	Serine 16
SERCA	Sarco(endo)plasmic reticulum calcium ATPase
SR	Sarcoplasmic reticulum
Thr17	Threonine 17
β-AR	β-adrenergic receptor

Abstract

Normal cardiac physiology largely relies on calcium handling in cardiomyocytes by a process called excitation-contraction coupling (ECC), in which the calcium pump, the sarco(endo)plasmic reticulum calcium ATPase (SERCA) and its predominant inhibitor, phospholamban (PLN), play important roles. Dysfunction in ECC can cause heart failure which is a leading cause of death worldwide with a five-year death rate of ~50%. It was reported in many early studies in heart failure that SERCA abundance and function is downregulated whilst PLN abundance remained unchanged. However, the levels of phosphorylated PLN (pPLN) are often noted to be downregulated and contributing to the reductions in SERCA activity. Gene therapy of SERCA has been demonstrated to be an effective therapeutic target in animal models of HF. However, this approach failed to make progress in multiple clinical trials. This study used a myocardial infarction ovine model that is comparable to human ischaemia reperfusion induced heart failure to determine SERCA, PLN and pPLN abundance in the remote and border regions of the infarcted left ventricle, and to investigate the hitherto overlooked area − the sub-cellular distribution of SERCA and PLN with high-resolution nanoscale STORM imaging. This study found that SERCA protein abundance has significantly increased in the remote region 20 weeks MI compared to control There was no change in PLN abundance, and a decrease in pPLN levels compared to control. These findings emphasize the importance of pPLN in heart failure pathogenesis which might explain why SERCA gene therapy was not effective. There was no change in either SERCA cluster size or distance after phosphorylation. However, this study also found PLN has a smaller distance between clusters after phosphorylation which is possibly due to PLN pentamerization. It would be intriguing to see whether this PLN redistribution is altered in heart failure in the future study, and if redistribution is observed, this might give a new therapeutic target in treating heart failure.

Declaration

I declare that this report entitled 'Sarco(endo)plasmic reticulum calcium ATPase and Phospholamban remodelling following myocardial infarction in an ovine model' is written and submitted by me under the supervision of Prof Andrew Trafford to the Division of Cardiovascular science of the University of Manchester for the award of Master of Philosophy degree of Cardiovascular science.

I declare that the animal model surgery and *in vivo* data were conducted by Dr Barbara Niort, Miss Olivia Johnstone, and Miss Agnieszka Swiderska and all the other research is my original work and all the data included are authentic. This report has not previously been used for any other purpose.

Copyright statement

regulations (see http://www.library.manchester.ac.uk/about/regulations/) and in the University's policy on Presentation of Theses.

Acknowledgement

First, I would like to thank Prof Andrew Trafford who provided me with the place in his lab and gave me all the guidance and support I need throughout the year and completing this report. I feel very lucky to be a part of the friendly and supportive group.

Second, I would like to thank Dr Lauren Toms and Dr Charlotte Smith who gave me indispensable support during the learning of STORM imaging and analysis which commit an important part of this report.

Third, I would like to thank Dr Barbara Niort, Miss Olivia Johnstone, Miss Charlotte Marris, and everyone else in Trafford lab who contributed to cell isolation and tissue collection, and Dr Katie Ryding who taught me the technique of Western blot. I would like to thank Dr Barbara Niort, Miss Olivia Johnstone and Miss Agnieszka Swiderska separately for setting up our sheep models and doing the surgeries.

Finally, I would like to thank my friends outside the lab who gave me mental support and discuss research techniques with me during my academic year while I am far away from home.

Chapter 1

General Introduction

1. Introduction

1.1 General introduction

In a normal heart, contraction of the cardiac myocyte is driven by the excitation-contraction coupling (ECC) process, where the electric action potential signal opens L-type Ca^{2+} channels (LTCC) which then trigger a calcium induced calcium release (CICR) of calcium from the ryanodine receptors (RyRs), increase the intracellular Ca^{2+} concentration and lead to cell contraction. Ca^{2+} is then removed by sarco(endo)plasmic reticulum calcium ATPase (SERCA) and Na^{+}-Ca^{2+} exchanger (NCX) and lead to relaxation. In a diseased situation, such as heart failure, the balance of the coupling is interrupted, and alteration could occur at any components of the coupling, i.e. the expression and distribution of the Ca^{2+} handling channels.

As a major Ca^{2+} handling protein, reduction of SERCA abundance had long been suggested to be a key player in heart failure pathogenesis (Eisner, Caldwell and Trafford, 2013). Indeed, recent experimental data in guinea pigs and sheep with adenoviral overexpression of SERCA2a showing improved contractility (Mariani *et al.*, 2011; Cutler *et al.*, 2012), however, the CUPID clinical phase 2 trial did not improve the clinical outcomes of patients with heart failure (Greenberg *et al.*, 2016). Although Ca^{2+} can be better eliminated from the cytosol during decreased SERCA2a activity/expression in heart failure state by compensational upregulation of NCX, it does lead to SR Ca^{2+} loss from the cell and exacerbation the impaired dysfunction (Li *et al.*, 2012), which makes NCX a less promising target for heart failure treatment. The predominant regulator of SERCA activity is PLN, which interact with SERCA to reduce its affinity to Ca^{2+}, and the inhibitory effect is removable through PLN phosphorylation (Tada, Kirchberger and Katz, 1975). PLN abundance, phosphorylation state and PLN:SERCA ratio had been found to be altered in heart failure and is still lacking evidence of the applicability of using PLN as therapeutic target. Last but not the least, RyRs distribution and Ca^{2+} release is also found to be change in heart failure (Macquaide *et al.*, 2015; Kolstad *et al.*, 2018) which is a relatively new research area and need more study to understand the relationship between RyRs and heart failure.

The mortality of heart failure is comparable to cancer, and the prognosis is not optimistic, with a five-year death rate of ~50% (Taylor *et al.*, 2019). Heart failure still remains incurable nowadays. Treatment could be developed based on understating the alterations of ECC components, and this thesis will be elucidating the current knowledge about SERCA, PLN and RyRs in heart failure, and focused to work on what has been overlooked.

1.2 Normal cardiac function

1.2.1 The electric contraction coupling

Normal cardiac contractility relies on calcium handling in the cardiomyocytes. Heart contraction is fulfilled by a process called excitation-contraction coupling (ECC) which takes charge of the calcium cycling in cardiomyocytes (Fig.1). ECC starts from action potentials generated from sinoatrial node (SAN) pacemaker regions and conduct through the atria before crossing the atrioventricular node and conducting via the His-Purkinge system throughout the ventricular myocardium (Bers, 2001). At the ventricular myocyte this electrical activity propagates along the cell surface and down a specific region that penetrates the cardiomyocytes called the T-tubule, with a distance of ~2μm (Page, 1978). The T-tubule forms a close apposition with the terminal of the sarcoplasmic reticulum (SR). This structure is termed a dyad. The role of T-tubule and dyad is important as Ca^{2+} sparks are more frequently observed around this structure (Shacklock, Wier and Balke, 1995), and ECC-related proteins are found to be assembled around T-tubule (Carl *et al.*, 1995). Moreover, detubulation (removal of T-tubule) by formamide can reduce Ca^{2+} current density and Ca^{2+} transient amplitude (Brette, Komukai and Orchard, 2002). The L-type Ca^{2+} channels (LTCC) that reside on the T tubule membrane is activated by the depolarization brought by the action potentials and when open allow a Ca^{2+} influx into the cell across the dyad. Opposite to the LTCC on the surface of the intracellular Ca^{2+} store, the sarco(endo)plasmic reticulum (SR) membrane is a cluster of intracellular Ca^{2+} release channels, the ryanodine receptors (RyRs). The Ca^{2+} entering the cell via the LTCC then triggers the synchronized opening of RyRs and release Ca^{2+} from the SR, generating a quantal Ca^{2+} release known as the Ca^{2+} spark (Cheng, Lederer and Cannell, 1993). This process is called calcium-induced calcium release (CICR) and will lead to a contraction of the cell as the combined Ca^{2+} entry and release gives rise to the systolic Ca^{2+} transient and provides the Ca^{2+} necessary for myofilament activation (Bers, 2001). The systolic flow

of Ca^{2+} is the basis of muscle contraction, and in myocytes the SR is the main provider of the Ca^{2+} needed for contraction (~ 74 % of the total requirement) in comparison to the extracellular influx (~ 26%) and cytosol Ca^{2+} in human (Bers, 2014). The released calcium will then be removed by SERCA as well as NCX (Reuter and Seitz, 1968; Lederer and Tsien, 1976) and will be restored into the SR or pump out of the cell respectively, and this step will cause muscle relaxation. Ca^{2+} removed by SERCA is the main route (~74%), this is also necessary as it balances with the Ca^{2+} flux in contraction. Around 25% of the Ca^{2+} is removed by NCX and the rest 1% through other slow mechanisms.

Generally, action potentials in the heart are self-generated due to the inherent pacemaker activity of the SAN but contraction can still be controlled by the sympathetic nerve with neurotransmitters, for example, the catecholamine family including adrenaline and noradrenaline, binding to β-adrenergic receptors (β-AR). This will release cAMP and upregulate PKA, which can phosphorylate LTCC and RyRs result in increased contractility. Another target of PKA is phospholamban (PLN), an inhibitor of SERCA, and phosphorylated PLN will lose inhibition on SERCA which will be discussed further in later sections. There are three different isoforms of β-AR found in cardiac myocytes: β_1-AR, β_2-AR and β_3-AR, although expression of β_3-AR in human heart is sparse and is currently considered to be negative inotropic (Gauthier *et al.*, 1998) in opposite to the other two. β_1-AR is the most predominant subtype expressed in human heart and is responsible for most of the inotropic effect evoked by catecholamine (Brodde, 1993), and is found to distributed on the entire cell surface and T-tubule, while β_2-AR is concentrated only at the T-tubule (Bathe-Peters *et al.*, 2021). This distinct distribution between β_1 and β_2 AR can be fundamental in maintaining healthy cardiac physiology, as β_2-AR redistribution towards cell surface is seen in heart failure rodents (Nikolaev *et al.*, 2010).

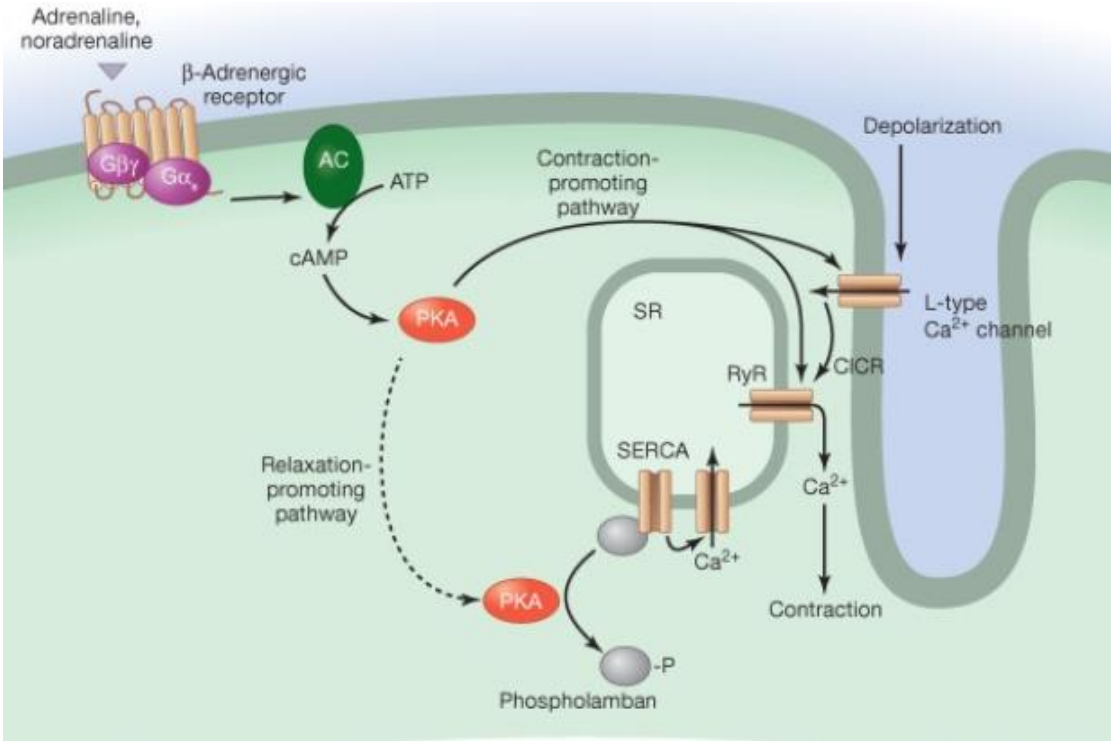

Fig.1 Excitation-contraction coupling. When action potential reaches the myocyte, depolarization cause the LTCC to open, triggers calcium-induced calcium release from RyRs. Calcium release causes contraction, followed by SERCA reuptake that causes relaxation. (Kuo and Ehrlich, 2015)

Looking more closely at the dyad, the distribution of the channel proteins is not random. RyRs are normally distributed in clusters and a group of clusters form a functional unit called the calcium release unit (CRU) (Fig.2). Similarly, LTCCs are also distributed as clusters and a cluster of LTCC associates with a CRU (RyRs cluster) to constitute a functional site of ECC, and the distance between LTCC and CRU, known as the dyadic cleft, is around 10-12 nm (Koh *et al.*, 2006). Approximately 10% of the NCX are found colocalized with RyRs clusters (Edwards *et al.*, 2018), however colocalization of SERCA and CRU is currently very poorly understand, and unpublished data from our lab suggests they are largely colocalized.

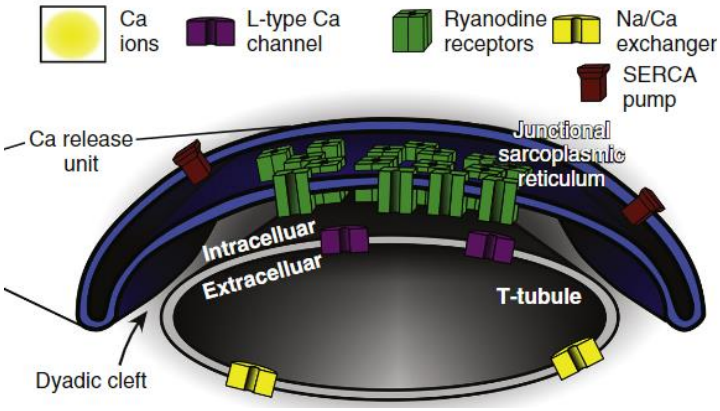

Fig.2 Protein distribution at the dyad. (Edwards et al., 2018)

1.2.2 Sarco/endoplasmic reticulum Ca^{2+}ATPase

SERCA is a P-type ATPase, which means it uses the energy from ATP hydrolysis to complete Ca^{2+} transportation. It is constituted by four domains, the Actuator domain, the Phosphorylation domain, the Nucleotide-binding domain and the Transmembrane domain. The transmembrane domain of SERCA contains 10 helical segments (M1-M10) which includes two Ca^{2+} binding sites (Tadini-Buoninsegni *et al.*, 2018). SERCA transforms between two states, E1 and E2, under the action of phosphorylation (Fig.3). During the event of muscle relaxation, SERCA starts with the E1 state that has a high affinity to Ca^{2+} and binds with two free Ca^{2+} from the cytosol. When phosphorylated by ATP, SERCA translocate the two Ca^{2+} towards the lumen of SR by transforming into the E2 state which has a low affinity of Ca^{2+}, therefore the Ca^{2+} ions are released. It then carries two protons in exchange and return to the E1 state and is now ready for the next cycle. SERCA is encoded by three genes from the same family, SERCA1, 2 and 3, and they together encode more than 10 isoforms of SERCA protein. These isoforms have tissue-specific development and distribution, in which SERCA2a is the majority type found in the cardiac myocytes (99%) (Lipskaia *et al.*, 2014) and will be the main focus of this study.

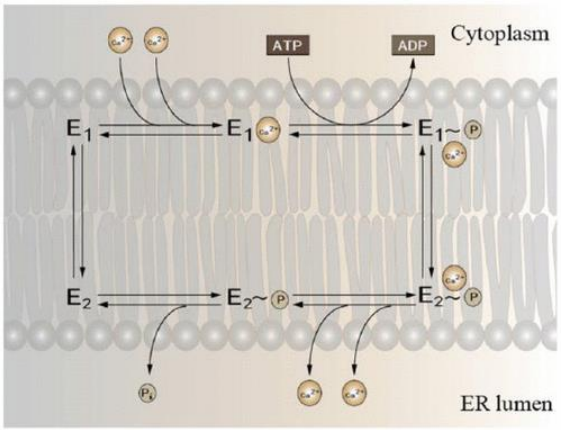

Fig.3 The mechanism of SERCA action. During relaxation, Ca^{2+} binds to SERCA and are transferred under the action of ATP and SERCA transformation. (Liu *et al.*, 2018)

1.2.3 Phospholamban

SERCA activity was initially related to phosphorylation events early in 1974, where Tada *et* al (1974) identified that SERCA activity (represented by Ca^{2+} uptake into lipid vesicles) is stimulated by cAMP and protein kinase A (Tada *et al.*, 1974). Later in 1975, the same group discovered a separatable, low-mass protein (22kDa) that received most of the phosphate during cAMP treatment, and further confirmed that the phosphorylation of this protein is related to the regulation of SERCA activity (Tada, Kirchberger and Katz, 1975). The name of phospholamban was given to this small protein, which means 'to receive phosphate'. In 1989, the exact function of PLN was clarified to be an inhibitor of SERCA in its dephosphorylated form, while phosphorylation relieves this inhibition and promotes increased SERCA affinity to Ca^{2+} (Sham, Jones and Morad, 1991). PLN is now identified as a pentameric protein formed from identical monomers, each monomer consists of 52 amino acids that contain 3 phosphorylation sites regulated by different protein kinase: 1. Serine10 by protein kinase C, 2. Serine16 (Ser16) by protein kinase A and 3. Threonine17(Thr17) by Ca+/calmodulin-dependent protein kinase II (CaMKII). It is believed that the Thr17 phosphorylation is a follow up step of Ser16 phosphorylation through interaction between the PKA and CaMKII pathway (Luo *et al.*, 1998)(Napolitano *et al.*, 1992), although some studies also suggested Thr17 could be phosphorylated independently. Ser16 phosphorylation is suggested to be capable to reach the maximum inhibition releasing effect(Chu *et al.*, 2000), while the importance of Thr17 phosphorylation is not entirely understood, and can be involved more in a pathophysiological state, like heart failure(Napolitano *et al.*, 1992).

A key question regarding the interaction with and functional inhibition of SERCA by PLN is the role of the monomeric and pentameric forms of PLN. In this regard, studies using mutant forms of PLN have led to the hypothesis that the PLN monomer acts as the active inhibitor of SERCA and the pentameric form is more of a reservoir, as mutation that stabilize the pentamer form would reduce the inhibitory effect of PLN while superinhibitory mutation was found to be devoid from pentamer form (Kimura *et al.*, 1997). This was also supported by structure study of PLN-SERCA interaction, in which it was found that PLN monomer is able to fit into a groove in SERCA formed by M2, M6, M4 and M9 in the transmembrane domain (Gustavsson *et al.*, 2013). The interaction site, however, is not close to the Ca^{2+} binding site, which means the physical

binding is not how PLN prevent Ca^{2+} from entering SERCA. It was found that PLN interact with SERCA in its E2 state, which as explained previously has low affinity to Ca^{2+} (Toyoshima *et al.*, 2003)(Akin *et al.*, 2013). By stabilizing SERCA in this state, PLN can lower the chance of Ca^{2+} entrance. This makes PLN an uncompetitive inhibitor that is removable when high concentration of Ca^{2+} is presented, and it would physically detach PLN from SERCA (Asahi *et al.*, 2000). Phosphorylation of PLN at Ser16 and Thr17 can also remove the inhibitory effect of PLN but has a different mechanism to high [Ca^{2+}]. Upon phosphorylation at the Ser16 site, PLN undergoes a conformational change meaning that it no longer docks with the inhibitory groove in SERCA although it still remains attached to SERCA (Asahi *et al.*, 2000, Gustavsson *et al.*, 2013)(Fig.4). Phosphorylation at Thr17 does not give a distinct conformational change as Ser16 that release PLN from the inhibitory groove according to a simulated model, therefore it's structural change might physically detach the PLN from SERCA (Sayadi and Feig, 2013), but still lack *in vivo* evidence. Phosphorylation of PLN can be removed by protein phosphatase 1 (PP1), given a reversible regulation of PLN on SERCA(Vafiadaki *et al.*, 2013).

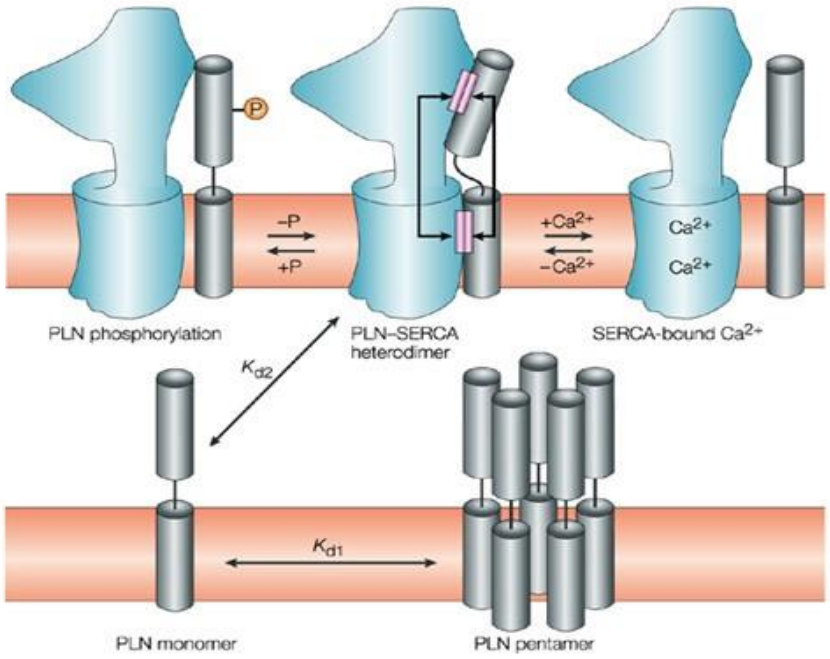

Fig.4 An overview of PLN-SERCA interaction under different conditions. When PLN monomer interact with SERCA and fit into the transmembrane groove, it inhibits SERCA activity. Phosphorylation of PLN, specifically at Ser16 site, triggers a conformational change that makes it non-inhibitory, while elevated Ca^{2+} concentration fully detaches PLN from SERCA. (MacLennan and Kranias, 2003a)

1.2.4 Ryanodine receptor's structure and organization in the heart

The RyRs is a large tetrameric protein formed from four identical monomers, each with a molecular mass of around 565 kDa (Tunwell *et al.*, 1996). The primary function of the RyRs is to act as a Ca^{2+} releasing channel for the SR and it is situated on the SR membrane closely opposed to the LTCC thereby forming the cardiac dyad. There are three isoforms of RyRs: RyR1, RyR2 and RyR3, and the most dominant form in cardiac muscle is RyR2. Immunohistological, studies have demonstrated that RyRs are mostly located in the z-line in cardiac cells and are grouped together forming clusters, each cluster function as a CRU. In adult mammalian ventricular myocytes, RyRs formed CRUs are predominantly found adjacent to a t-tubule forming a couplon with LTCC. However, some RyRs are not opposed to LTCCs or surface membranes and are referred to as 'orphaned' RyRs (Franzini-Armstrong, Protasi and Ramesh, 1999; Song *et al.*, 2006).

Typically, upon electrical excitation via the action potential, Ca^{2+} is released several or all RyRs in a cluster and is 'visible' under a confocal microscope as the so-called Ca^{2+} 'spark' (Cheng, Lederer and Cannell, 1993). Importantly, RyRs generally has a very low opening rate in a resting cell with a rate of ~0.0001 openings per second (Cheng, Lederer and Cannell, 1993), but the opening probability of RyRs is largely affected by $[Ca^{2+}]$ in the SR and within the cleft (Sato and Bers, 2011). The majority of the Ca^{2+} releasing event in cardiac muscle is evoked sparks from RyRs, where Ca^{2+} influx from the LTCC will increase $[Ca^{2+}]$ in RyRs cleft that bind to and open RyRs and lead to a large efflux of Ca^{2+} from the SR store, this efflux can furthermore increase the $[Ca^{2+}]$ in cleft and triggers more neighbouring RyRs clusters, producing a long-lasting Ca^{2+} rise such that the summation of Ca^{2+} sparks gives rise to the systolic Ca^{2+} transient. This process, referred as CICR, is the main responsible source for cardiac myocytes contraction.

Additionally however, Ca^{2+} sparks can also give rise to a pro arrhythmic substrates, the Ca^{2+} wave which underpins triggered activity in the intact heart (Mattiazzi *et al.*, 2015). For simplicity these Ca^{2+} sparks are referred to as spontaneous Ca^{2+} spark, which also highlights the lack of requirement for Ca^{2+} entering from LTCC. This independence of external Ca^{2+} entry was verified through removal of extracellular Ca^{2+} and LTCC antagonist application (Cheng and Lederer, 2008). The occurrence of spontaneous Ca^{2+} spark is dependent on $[Ca^{2+}]$ in cytosol and SR lumen, and high luminal and cytosol

concentration will prompt RyRs opening and increase Ca^{2+} sparks frequency. The formation of spontaneous Ca^{2+} spark seems to have a threshold that when SR Ca^{2+} is reduced to an extent, spontaneous Ca^{2+} spark can be fully abolished(Sato and Bers, 2011). It is also shown that the arrangement of RyRs within a cluster can affect the open probability of the cluster and the initiation of sparks, which is defined by the maximum eigenvalue of the adjacency matrix of the cluster (Walker *et al.*, 2015).

The Ca^{2+} spark is a stochastic event which usually self terminates. Here it is suggested that Ca^{2+} spark termination is determined by the residual Ca^{2+} within the SR as sparks were found to stop at a similar SR [Ca^{2+}] and independent of the starting Ca^{2+} concentration within SR (Zima *et al.*, 2008). However, the same paper also found that the sparks would slowly and eventually terminate even at a constant SR [Ca^{2+}], suggesting that it could be otherwise regulated by the amount of Ca^{2+} efflux or [Ca^{2+}] in cleft or possibly via flux dependent closure of the channels. Another study also suggested that the Ca^{2+} flux across the RyRs itself may also cause spark termination rather than depletion of the SR content (Guo, Gillespie and Fill, 2012).

Despite of Ca^{2+} spark, there is another Ca^{2+} activity in cells that is too small to be visible under conventional confocal microscope, termed as Ca^{2+} leak. It can happen when only one RyR or several are opened but the current is not strong enough to trigger a spark in the CRU (Fig.5). It can also be released from dissociated RyRs that is not presented in clusters (Williams *et al.*, 2011). Similar to spontaneous Ca^{2+} spark, Ca^{2+} leak can also be increased when there is SR Ca^{2+} overload. Interestingly, Ca^{2+} leak doesn't require a threshold to present and can still be detected at low SR Ca^{2+} (Zima *et al.*, 2010).

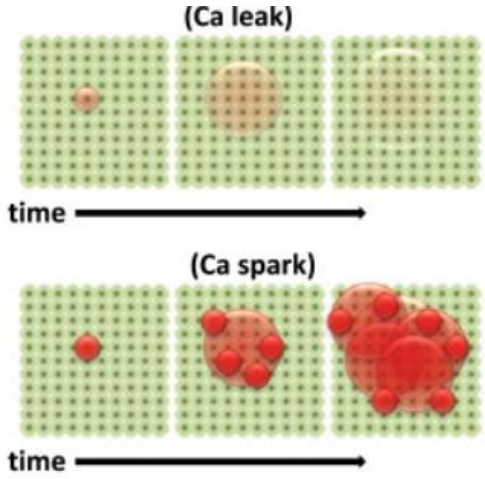

Fig.5 An illustration of Ca^{2+} leak (top) where a weak Ca^{2+} efflux is generated at one RyR, and a Ca^{2+} spark (bottom) where a strong Ca^{2+} efflux is produced and trigger a synchronized release of Ca^{2+} from other neighbour RyRs. (Sato and Bers, 2011)

1.2.5 Phosphorylation targets in cardiac excitation contraction coupling

Adrenergic effects triggered by catecholamine activation of β-adrenergic receptors modulates the contractility of the cardiac myocytes to affect an increase in contraction (inotropy) and the rate of relaxation (lusitropy). In brief, this is achieved by activation of a canonical downstream signalling pathway. β-adrenergic receptor activation activates adenylate cyclase via a stimulatory GTP-binding protein ($G_{\alpha s}$) and produces cAMP. cAMP then activates protein kinase A (PKA) which goes on to phosphorylate a number of downstream targets producing the classical inotropic and lusitropic responses. With direct relevance to this programme of work, PKA phosphorylates LTCC subunits which increases their open probability and opening time upon activated by an action potential, therefore increasing Ca^{2+} influx into the myocyte and causing a larger release of Ca^{2+} from the SR. PKA also phosphorylates Serine 2808 on RyRs which increase their open probability; albeit whether this causes a maintained increase in systolic Ca^{2+} is debated (Eisner *et al.*, 2010; Shan *et al.*, 2010). This would increase the Ca^{2+} efflux from the SR store.

In addition, PLN is also phosphorylated by PKA at its Serine 16 site. This phosphorylation will release the inhibitory effect of PLN on SERCA, therefore increase the activity of SERCA and Ca^{2+} restoration. Overall, PKA phosphorylation increase the Ca^{2+} transient in cardiac cell without affecting the net concentration, increase the contractility and relaxation upon β-adrenergic receptors activation. As noted above, this phosphorylation may also result in a change to the monomer to pentamer ratio of PLN and thus overall inhibition of SERCA activity.

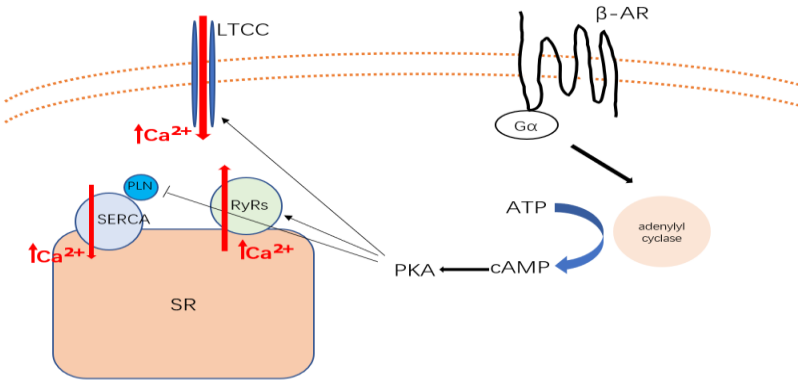

Fig.6 β-AR mediated phosphorylation site in cardiac myocytes. When β-AR being activated by agonist binding, Ga subunit will activate adenylyl cyclase, increase cAMP and PKA. PKA phosphorylation will increase LTCC and RyRs activity, release PLN inhibition on SERCA thus increase SERCA activity, and overall increase contractility.

1.3 Cardiac dysfunction

1.3.1 Heart failure

Heart failure, also known as congestive heart failure, is a condition where the blood ejected from the heart cannot meet the metabolic demands of the body. This will cause the patient to feel fatigued and short of breath, and insufficient blood supply will lead to damage to other body organs with time (Cohn, 1996). Heart failure is currently affecting ~920,000 people in the UK (Context | Chronic heart failure in adults: diagnosis and management | Guidance | NICE, 2021) and 26 million worldwide (Savarese and Lund, 2017). High morbidity meaning a high proportion of medical expenditure, and the prevalence is still rising due to increasing ageing and obesity as common risk factors for heart failure (Rodgers *et al.*, 2019; Powell-Wiley *et al.*, 2021). Given the broad range of risk factors for HF and their interdependence the actual cause can be hard to determine, for example, cardiac hypertrophy, resulting from high blood pressure, can lead to the pathogenesis of heart failure; on the other hand, hypertrophy can also be a consequence of heart failure as the heart as a compensatory mechanism to increase contractility, therefore increase the blood flow (Dieterle *et al.*, 2005a). The main causes of heart failure include coronary heart diseases resulting in ischaemic damage which is typically due to underlying atherosclerotic artery disease (Gheorghiade and Bonow, 1998). Other common causes of heart failure include: hypertension; cardiomyopathies of genetic origin (dilated, hypertrophic) and some arrhythmia syndromes (McMurray and Stewart, 2000; Morita, Seidman and Seidman, 2005). Heart failure is typically a chronic disease with progressively worsening symptoms and ultimately causing death in many patients due typically to either pump dysfunction or sudden arrhythmic cardiac death (McMurray and Stewart, 2000). Importantly, whilst a disease of the heart, HF tends to involve multiple organs leading to systemic illness (Alsafwah *et al.*, 2007). Importantly, five-year survival rates of patients with heart failure are worse than many of the typical cancers highlighting the need for better mechanistic understanding to help identify potentially more efficacious novel therapeutic approaches.

1.3.2 Heart failure subtypes, aetiology, and consequences

As insufficient of blood is pumped out by the heart in heart failure, the left ventricle is commonly found to be enlarged. Initially the increase in size and wall thickness (hypertrophy), via Laplace's Law, helps normalise wall stresses and supports

compensated cardiac function. However, as the disease inevitably progressed, and these initial compensatory changes failed this led to the change in the left ventricle volumes becoming considered as typically characteristic of heart failure patients. A reduction in left ventricle ejection fraction, which is the volumetric fraction of blood being pumped out by the left ventricle in each contraction, had long been introduced to be a classification of heart failure since 1980s, and used as an index for patient recruitment in clinical trials (Savarese *et al.*, 2021). Heart failure patients with normal ejection fraction were soon discovered in 1984 (Dougherty *et al.*, 1984), but not largely enrolled in clinical trials up till now and left with insufficient treatment strategy (Yancy *et al.*, 2013). The major two types of heart failure are now classified as heart failure with reduced ejection fraction (HFrEF) and heart failure with preserved ejection fraction (HFpEF), where their phenotype, aetiology, treatment, and prognosis can be largely different. However, a more intermediate classification is now emerging where patients are described as having mid-range ejection fraction (HFmrEF). The American College of Cardiology/American Heart Association first recognized patients with left ventricle ejection fraction between 41% and 50% as "borderline" HFpEF in 2013 (Yancy *et al.*, 2013), then in 2016, the European Society of Cardiology classified HF with ejection fraction between 40 and 49% as a new phenotype HFmrEF to encourage research input into the new area (Ponikowski *et al.*, 2016). The precise categorization of HF according to ejection fraction is clinically meaningful, for example, trails that failed to show benefits in general HF can have positive outcome in sub-group (Solomon *et al.*, 2020).

1.3.3 Calcium-handling proteins variation in heart failure

As early as 1987, Gwathmey *et al.* had already discovered the relationship between calcium-handling protein dysfunction and heart failure (Gwathmey *et al.*, 1987). By using different blockers targeting aspects of the processes involved in cardiac excitation contraction coupling, they've hypothesised that the change in Ca^{2+} transient (reduction and slowing) observed in heart failure arose from two components: either the amount of Ca^{2+} going out from the SR, or the ability of Ca^{2+} reuptake into the SR. Subsequently, it was discovered that the rate of $[Ca^{2+}]$ decline during diastole was much slower in isolated ventricle cells in heart failure patients in comparison to normal heart(Beuckelmann, Näbauer and Erdmann, 1992), which support the latter hypothesis made by Gwathmey *et al.*, suggesting that the proteins responsible for Ca^{2+} removal could be altered in heart failure. Based on a wide range of subsequent experimental

studies our understanding today both SERCA and PLN play key parts as part of the responsible proteins underlying the disease.

1.3.3.1 SERCA change in heart failure

Reduction of SERCA abundance and activity with aging is reported in human studies and animal models, and is thought to be at least partly responsible for the decreasing cardiac function in ageing (Lakatta and Sollott, 2002; Qaisar *et al.*, 2021). These studies have been supported by studies employing SERCA knock out mouse models where it was found that heterozygous knock out resulted in decreased cellular contractility, coupled to reduced responsiveness to catecholamine stimulation. Furthermore SERCA knockout were more susceptible to develop heart failure (Fig.7) (Talukder *et al.*, 2008; Andersson *et al.*, 2009). However, SERCA knockout was found to have protective effect towards arrhythmias and the authors suggested it could be due an increase of calcium efflux from NCX and reduction in SR calcium load (Edwards *et al.*, 2021), but increase in NCX activity can also be susceptible to arrhythmia itself (discussed later in this section) and RyRs remodeling might be contributing to the protective effect.

Additionally, SERCA mRNA expression, protein abundance and function have all been found to decrease in various models of heart failure. (Mercadier *et al.*, 1990; Hasenfuss *et al.*, 1994; Currie and Smith, 1999). Whilst it is a generally held view that SERCA activity and or expression/abundance is reduced in heart failure, this is not always the case. Whilst it is currently largely agreed that SERCA abundance is decreased in heart failure, there are studies reporting no change in the protein level, but decreased in SERCA activity in human heart failure (Schwinger *et al.*, 1995). A possible explanation for these seemingly discrepant observations may be provided by considering the role that alterations in the SERCA to PLN ratio and PLN phosphorylation status have (see section 1.3.3.2).

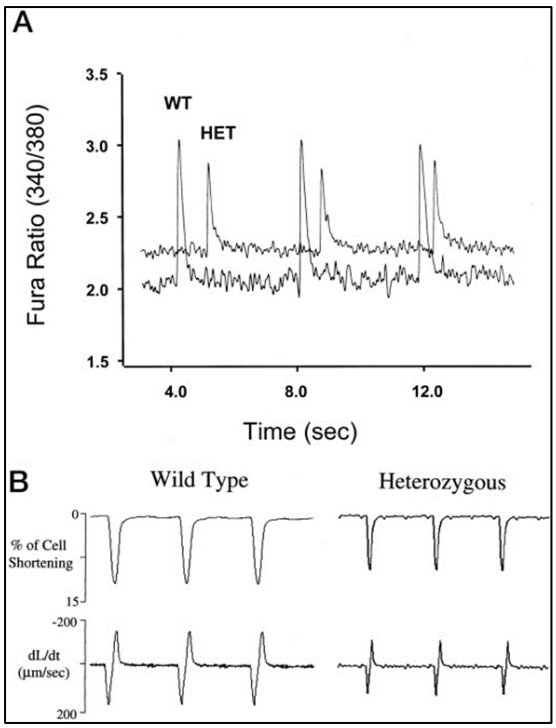

Fig.7 Experiment results showing a heterozygous SERCA knock out mice would have weaker Ca^{2+} transient (A), lower rate of cell shortening and relengthening (B) from Ji *et al.*

(Ji *et al.*, 2000)

There is also indirect consequence brought by SERCA depression. NCX upregulation had been found in compensation to the decrease of SERCA, which would lead to the accumulation of sodium intracellularly, and worsens the heart failure (L*i et al*, 2012). As NCX transfer 3 Na^+ intracellularly in exchange of 1 Ca^{2+}, this will cause a inwards current that prolong the action potential and early afterdepolarization (Huang, Song and Qu, 2018), therefore increasing NCX activity can be predispose to arrhythmias. Indeed, it was found that heterozygous knockout of the NCX can suppress afterdepolarization (Bögeholz *et al.*, 2015). In conclusion, SERCA expression and activity is highly related to cardiac physiology.

1.3.3.2 Phospholamban changes in heart failure

In animal models, ablation of PLN increases SERCA activity, enhances contractility and prevents development from heart failure (MacLennan and Kranias, 2003a). Importantly, despite its inhibitory effect on SERCA, the expression level of PLN is generally either unaltered or even decreased in heart failure (Bhupathy, Babu and Periasamy, 2007). However, the typically greater decrease in SERCA levels resulting in a decreased ratio in SERCA: PLN which would result in a further and enhanced inhibition on SERCA thus contributing to the overall pathophysiology of heart failure. The impact of increasing the SERCA to PLN ratio is exemplified by comparison of the SERCA to PLN ratio between the atria and ventricles and how this affects the kinetics

of the systolic Ca^{2+} transient (Walden, Dibb and Trafford, 2009). Here the lower SERCA to PLN ratio in the ventricle arising from the 3-fold higher PLN mRNA expression in the ventricle versus the atria is at least part of the reason why ventricle has lower contractility than the atria (Koss, Grupp and Kranias, 1997, Walden, Dibb and Trafford, 2009).

However, the above approach remains too simplistic, and it is important to also consider the phosphorylation status of PLN as this markedly affects SERCA activity (see Section 1.2.3). Notably, in heart failure the levels of phosphorylated PLN (pPLN) were reported to be downregulated, which would result in more PLN actively function on SERCA inhibition (Schmidt *et al.*, 1999; Schwinger *et al.*, 1999; Briston *et al.*, 2011). Thr17 phosphorylation was also found to be independent of Ser16 in a pathologic heart and could be a culprit in causing heart failure (MacLennan and Kranias, 2003b). Taken together, the level of pPLN and the ratio of SERCA: PLN are critical factors in altering cardiac physiology.

1.4 Current therapeutic strategies for heart failure targeting cellular calcium dysfunction

Heart failure is a non-curable disease currently. Whilst current optimal treatment can improve cardiac muscle function and delay mortality it cannot reverse deleterious changes that have already occurred and generally only act to only slow down the disease progression. Also, treatment mainly only aims at eliminating symptoms, for example, inotropic drugs that can increase heart contractility but overlook the underlying cause of the heart failure. Symptom targeting drugs might however lead to long term side effects, for example, inotropic drugs increases the risk of arrhythmias and mortality (Toma and Starling, 2010). Inotropic drugs such as adrenergic receptor agonists and PDE inhibitors, enhance SERCA2a function by increasing PLN phosphorylation. However, the overall enhancement of PKA activity phosphorylates many other targets including LTCCs and RyRs. This can result in the increase of SR Ca^{2+} content and leads to an increased tendency of SR Ca^{2+} leakage, resulting in delayed afterdepolarization and elevated probability to arrhythmia (Sikkel *et al.*, 2014). The situation will be even more adverse in heart failure patients who are already prone to arrythmia due to e.g. elevated intracellular sodium levels. Additionally, there is substantive evidence for drugs such as the synthetic catecholamine dobutamine and PDE3 inhibitor milrinone increasing mortality in heart failure (O'Connor *et al.*, 1999;

Packer *et al.*, 2010). Given these limitations of drugs aimed at increasing cardiac function via increasing cAMP levels that would affect a wide range of proteins, alternative approaches may therefore stem from specifically targeting SERCA, PLN and SERCA-PLN ratio which may increase contractility with less side effects, for example, gene therapy of SERCA and PLN, or other regulatory protein including PP1.

1.4.1 SERCA as therapeutical target

As explained previously, inotropic drugs and other non-specific, symptom-targeting drugs can have deleterious long-term effects when used as therapies for heart failure, which potentially makes SERCA a more promising therapeutic agent with inotropic properties with which target for heart failure treatment. Moreover, as SERCA isoforms are distributed in a tissue-specific manner, a treatment focusing on SERCA2a and thus being cardiac specific would potentially reduce the likelihood of unwanted systemic side effects. SERCA gene therapy had been demonstrated to be successful in preclinical animal models (Mariani *et al.*, 2011; Cutler *et al.*, 2012), however, when moving on to clinical trials, the results were not encouraging. The first human Phase I trial called the Calcium Upregulation by Percutaneous Administration of Gene Therapy in Cardiac Disease (CUPID1) was conducted on a small cohort of heart failure population (10 patients; Jaski *et al.*, 2009). Promising outcomes were given with improvement on multiple cardiac parameters and these findings propelled the initiation of the Phase II CUPID1 trial. The results from Phase IIa and a 3-year follow-up report of CUPID1 also agreed with the safety and benefit of AAV1/SERCA2a in human heart failure (Jessup *et al.*, 2011; Zsebo *et al.*, 2014) and further prompted the CUPID2 clinical trial which is a PhaseIIb trial including 250 patients from different countries. However, the CUPID2 trial revealed no improvement in cardiac outcomes compared to placebo (Greenberg *et al.*, 2016). The negative outcome from CUPID2 trail could be due to low efficiency in AAV1/SERCA2a transfer in human, where only a small portion of the heart tissue were expression the AAV1 transferred SERCA2a (Greenberg *et al.*, 2016). The lack of benefit in the interim outcomes of CUPID2 resulted in the premature termination of the trial and suspension on patient recruitment of two other clinical trials, AGENT-HF and SERCA-LVAD. These two curtailed trials with low participants number, in the end, failed to show any benefit of SERCA gene therapy (Hulot *et al.*, 2017; Lyon *et al.*, 2020).

1.4.2 Phospholamban as therapeutical target

As the predominant regulator of SERCA, PLN has logically spawned interest as a potential therapeutic target for the management of heart failure. A targeted ablation of PLN in the heart leads to an increase SERCA activity by increase affinity to Ca^{2+} and SR Ca^{2+} content and thus contractility (Luo *et al.*, 1994) and is therefore suggestive of potential therapeutic value. However, multiple studies have reported potentially adverse effects on cardiac morphology and function which would not confer useful benefit in heart failure, these negative aspects stem from PLN ablation leading to the heart becoming hypertrophic and a decrease in cardiac contractility (Shanmugam *et al.*, 2011). Additionally the genetic deletion of PLN in conjunction with heart failure models in mice revealed that absence of PLN does not prevent heart failure (Song *et al.*, 2003; Valverde *et al.*, 2019). A naturally occurring human PLN loss-of-function mutation agrees with these mouse model findings inasmuch as the absence of PLN leads to heart failure and premature mortality (Haghighi *et al.*, 2003). Therefore, inhibiting PLN function instead of removing PLN may be a better strategy, and evidence had shown that gene therapies interrupting PLN-SERCA interaction, increasing PLN phosphorylation and inhibiting PP1 activity (and thus maintaining PLN phosphorylation) all have a positive effect in improving calcium handling and contractility without having adverse pathological outcomes in preclinical models (Iwanaga *et al.*, 2004; Dieterle *et al.*, 2005b; Watanabe *et al.*, 2017). Importantly, these results are yet to be confirmed in humans.

1.5 Subcellular distribution and STORM imaging

1.5.1 Insight brought by RyRs cluster distribution and sparks formation

Super-resolution imaging study had given a lot more in depth understanding into RyRs in recent years, for example, size and distribution of RyRs in clusters (Hou *et al.*, 2015). Multiple studies had agreed that the average amount of RyRs in a single cluster (CRU) is roughly around 100 (Chen-Izu *et al.*, 2006; Cheng and Lederer, 2008), and the actual size of the clusters can vary a lot in cardiac myocytes, from 30 to 260 RyRs per cluster (Franzini-Armstrong, Protasi and Ramesh, 1999). Cluster with a size of ~10 RyRs was found to be enough to trigger a maximum Ca^{2+} spark (Fig.7). The size of clusters is linked with the frequency of Ca^{2+} sparks (Galice *et al.*, 2018), i.e., smaller clusters that would have less spontaneous leak would trigger less sparks, the frequency would increase with the cluster size gradually until there is a higher level of spontaneous sparks and leak of Ca^{2+} from the SR that depletes the SR of Ca^{2+}, and leads to a low SR

[Ca^{2+}] which would limit spark formation and reduce the frequency of Ca^{2+} spark formation. However, when increase the cluster size to the maximum, the number of RyRs spontaneous sparks and leak will also increase that lead to a the high [Ca^{2+}] in the cleft, and result in more frequent Ca^{2+} sparks (Fig.8). Therefore, maintaining an appropriate level of RyRs cluster size and packing density (arrangement) is an important consideration. To this end it is notable that increased heterogeneity of RyRs clusters is indeed observed in pathological conditions such as heart failure (Macquaide *et al.*, 2015; Kolstad *et al.*, 2018), and is associated with an increase in the sparks frequency which can cause arrhythmia due to delayed afterdepolarization (Xie *et al.*, 2019; Kistamás *et al.*, 2020).

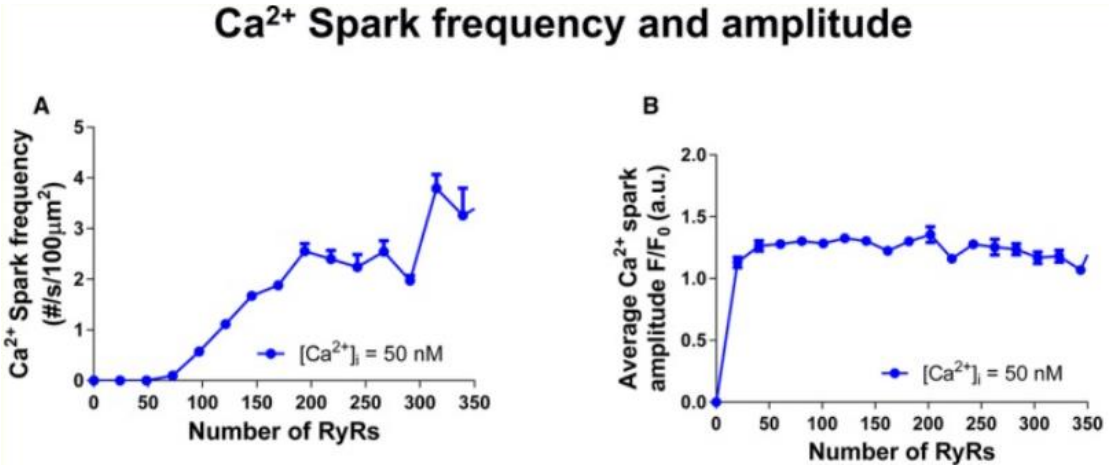

Fig.8 Ca^{2+} spark frequency and amplitude in relationship to number of RyRs in cluster. (Galice *et al.*, 2018)

More super-resolution study had revolved the gating mechanism of single RyR2 protein by recognizing the gating amino acids (Peng *et al.*, 2016), the relationship between the arrangement of RyRs within the clusters and cluster opening probability (Walker *et al.*, 2015), and even more, the reorganization of RyRs under pathological conditions (Kolstad *et al.*, 2018; Hadipour-Lakmehsari *et al.*, 2019). With the nano-scale research gradually became abundant in RyRs, it also brings insight of using this technology in other Ca^{2+} handling protein.

1.5.2 Current understanding of SERCA and PLN subcellular distribution

The more widely available data regarding the impact of sub cellular RyRs distribution highlights the importance of considering the nanoscale architecture of ion channel distribution in disease pathophysiology. In stark contrast to the situation regarding RyRs nanoscale distribution in health and disease, there is limited research focused on

the subcellular distribution of SERCA and PLN which is somewhat surprising given their central role in controlling cardiac function in health and disease.

Available immunohistological evidence indicates that both SERCA and PLN reside in the SR membrane with some literature also suggesting that SERCA is distributed as a longitudinal SR protein (Lipskaia *et al.*, 2014). However, confocal images had shown that SERCA and PLN localizes transversely and continuously throughout the cardiac cell and is likely to be near the Z line (Wu *et al.*, 2016). Furthermore, unpublished data from our own laboratory had shown that with a super-resolution imaging method, stochastic optical reconstruction microscopy (STORM) imaging, SERCA appears to localize predominantly on the Z line with minor distribution in between Z lines, and the distribution is not continuously but forms discrete cluster like groups (Fig.9). PLN also sits close to SERCA and shares a similar distribution pattern with it under these conditions. Together this suggests that SERCA and PLN can also have the 'clustering features'. Despite the novel discovery itself, the distribution pattern of SERCA also raises the question of whether this pattern and the morphology of protein clusters would change in physiological and pathological conditions, such as following acute β-adrenergic stimulation and in disease conditions such as heart failure. Considering the bottle-neck situation in the SERCA gene therapy field, research on SERCA redistribution following heart failure might point out a new direction in heart failure treatment.

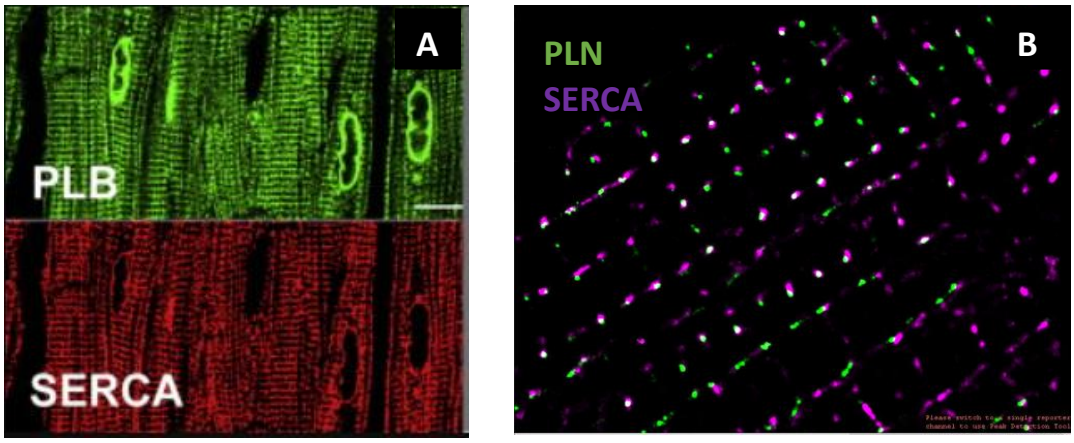

Fig.9 (A) Confocal image from Wu *et al.*, 2016 showing PLN and SERCA transversely distributed on Z line throughout the cell. (PLB is the same as PLN.) (B)STORM image taken by author showing PLN and SERCA colocalized together.

1.5.3 STORM imaging with TIRF

Based on the findings from RyRs clustering using nanoscale super resolution imaging modalities it is imperative that the sub-cellular distribution of SERCA and PLN be evaluated. To achieve this, a number of methodologies are now available which overcome the diffraction limited resolution of conventional light microscopy imaging methodologies and resulted in the Nobel prize for Chemistry being awarded to Hell and colleagues in 2014. Given its utilisation in this programme of work, this section will specifically review Stochastic Optical Reconstruction Microscopy (STORM).

STORM is a super-resolution imaging technique which by bathing the fluorescent-conjugated specimen in an oxygen-scavenging buffer, the fluorophores randomly switch between the light (photon emitting) and dark state, and each time when an image is taken, only the fluorophores in light state will be recorded. After taking a serial of images, they will be reconstructed together (Fig.10). By applying a Gaussian distribution to the emitted 'blink' profile and factoring in the optics of the system it is possible to localise the position of the emitting fluorophore to < 20 nm axial resolution and thus obtaining a ~ tenfold improvement in spatial resolution over confocal microscopy methods (Xu, Ma and Liu, 2017). This level of localisation accuracy and resolving power is well-suited to determining dyadic protein distribution given the RyR tetramers 29 * 29 nm dimension and ~ 12 nm dyadic cleft.

STORM is also equipped with TIRF (Total Internal Reflection Fluorescence) microscopy during usage. The application of TIRF restricts detection of the excitation pathway and thence emission and detection of fluorophores in the specimen. This is done by a total reflection of the excitation light when traveling through the cover glass, due to the generation of evanescent wave when get in touch with the liquid media (Fig.10). Only the fluorophores at the bottom of the specimen that is close to the cover glass would therefore be activated, which can eliminate the background noise from other layers.

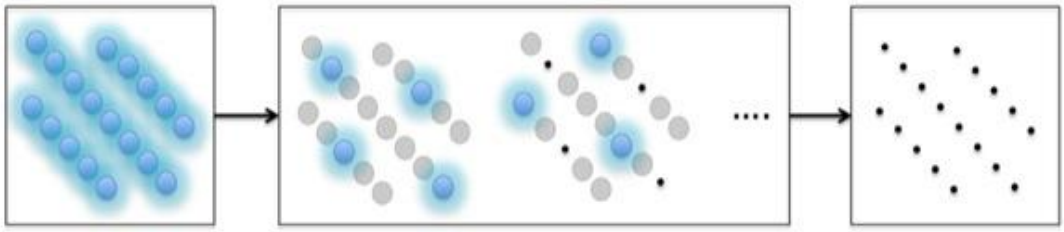

Fig.10 Illustration of STORM imaging mechanism. Fluorophore-labelled target will stochastically go into on/off state, and a series of pictures would be taken and reconstructed together at the end of imaging.

(*Part 2: The Who's Who of Super Resolution Microscopy - Single Molecule Localisation techniques - Bitesize Bio*)

1.6 Hypotheses

Bases on the mechanisms of E-C coupling and the pathogenesis of heart failure expounded in the previous sections, the hypothesis of this study are:

1. Protein abundance of SERCA and PLN would be altered in the condition of post-MI heart failure, where SERCA abundance would decrease, and PLN would increase. Phosphorylation of PLN would also be altered in a downregulated manner, therefore inhibit SERCA activity.
2. Sub-cellular distribution between SERCA and PLN would be remodelled after β-Adrenergic stimulation and post-MI.

1.7 Aims

From the current understanding of SERCA and PLN, it could be seen that they play fundamental role in operating a normal E-C coupling to maintain cardiac muscle contraction, and it is very common to find their function to be altered in heart failure. Currently, there is disagreement in whether their mRNA expression and/or protein abundance are changed in disease. The lack of nanoscale imaging data on SERCA PLN distribution in health and disease also presents challenges for understanding how their function may alter in disease. Together these factors may act as a limitation to fully understanding their role in health and potential approaches to restore their function in disease. Such factors may be germane to the failure of the SERCA gene therapy trial failing to show overall clinical benefit.

As such, the subcellular distribution of SERCA and PLN remained overlooked, and from the studies done on RyRs which shows that protein clusters sizes could regulate the function pattern, it is possible that the same features can be identified from SERCA

and PLN, and any novel finding might be able to point out a new therapeutic target for heart failure treatment.

Therefore, the aim of this study includes two parts:

1. To verify the protein abundance of SERCA, PLN and pPLN in left ventricle using a myocardial infarction ovine heart failure model;

2. To investigate the subcellular distribution of SERCA and PLN by comparing between control and myocardial infarction animals before and after β-Adrenergic stimulation using STORM imaging.

Chapter 2

General Methods

2. Methods

2.1 The applicability of ovine model

Mice models are extensively used in scientific study due to the lower expense and high reproduction rate and this is no exception in cardiovascular research. However, despite the high comparability of the anatomy and development of mice and human heart, there are also some key differences. Mice has a much higher resting heart rate between 500-600 beats/min(bpm) while in human it is 60-90 bpm, and mice also has a short action potential and in ventricle action potential there is a less significant plateau stage. SERCA is more predominant in conducting Ca^{2+} in rat and mice which can take up to ~90% during relaxation, and correspondingly SR Ca^{2+} release would also take ~90% of the total calcium influx during stimulation (Li *et al.*, 1998; Bers, 2000). In contrary, sheep, as a large mammal animal model, has closer body weight and heart weight to human and shares similar cardiac physiology to human, including structure, heart rate ((60–120 bpm) and blood pressure (Camacho *et al.*, 2016). Moreover, calcium removal during relaxation is estimated to rely more on SERCA in sheep (~81.5%) which is more comparable to human (~74%) (Dibb *et al.*, 2004), this is especially important to this project as it focuses on calcium handling proteins.

2.2 Ethical Approvals

All procedures involving the use of animals were performed in accordance with The United Kingdom Animals (Scientific Procedures) Act, 1986 and European Union Directive 2010/63. Institutional approval was obtained from The University of Manchester Animal Welfare and Ethical Review Board. The reporting of animals in experimental studies accords with the ARRIVE (Animal Research: Reporting of In Vivo Experiments) guidelines(*Home | ARRIVE Guidelines*).

2.3 Animal model

Young female Welsh Mountain sheep aged within 18 ± 6 months (age of weaning and sheep can live independently at this stage) were randomly allocated for MI induction surgery or as controls. Animals were kept in groups and held in a 12-hour light/12-hour dark cycle. MI surgery was conducted by Dr Barbara Niort, Miss Olivia Johnstone, and Miss Agnieszka Swiderska. Before surgery, anaesthesia was induced and maintained by isoflurane inhalation (~ 2.5% v/v), once the sheep is under anaesthesia, Metacam was used as pain relief (0.5 mg/kg IM) and Terramycin (used as antibiotic (20 mg/kg

SC) were administered. During surgery, MI was induced in sheep by inflating an angioplasty balloon after the 2nd diagonal branch of the left descending coronary artery. The balloon remained inflated for 90 minutes occluding blood flow distal to the balloon. During this time, the presence of myocardial infarction was confirmed by closely monitoring ECG parameters through the presence of ST elevation, which usually were observed within minutes of the occlusion. Additional arrhythmic ventricular activity could be seen approximately 30 - 40 minutes into the occlusion, including ventricular fibrillation. All MI animals were also implanted with an implantable cardiac defibrillator (right ventricle) prior to MI induction and 35 J defibrillation shocks administered if animals developed ventricular fibrillation. MI was also confirmed by measuring serum levels of cardiac troponin I. Following the occlusion, troponin levels rose as observed in clinic (see section 3.2). MI sheep were left to recover in separate pen but in close visible proximity to the rest of the group. Animals were humanely killed at two time points post-MI of 8 weeks and 20 weeks for experimental purposes. No surgical procedures were carried with control group of animals.

2.4 Animal euthanasia

The euthanasia of control and MI sheep were carried out as per the approved schedule 1 protocol in accordance with ABPA regulations with an anaesthetic overdose followed by permanent cessation of circulation. 10,000 IU IV heparin is administered via a peripherally placed 21G cannula in the control animals and 20,000 IU in the MI animals 2 minutes prior to euthanasia to prevent blood clot forming in vessels that might block the circulation and affect the quality of later cell isolation. Euthanasia was achieved by an injection of sodium pentobarbitone 20% solution (1mg/kg) (Animalcare, UK). Euthanasia was confirmed with the absence of blink reflex and cessation of circulation. A thoracotomy was performed to remove the heart. The heart would be placed in a Ca^{2+} free isolation solution (see section 2.5).

2.5 Cell isolation

The isolated heart was cut at 1cm below the atrio-ventricular groove to separate the atria and the ventricle. The left ventricular free wall was perfused by cannulation of the left anterior descending artery and the cannula was connected to the Langendorff system. The Ca^{2+} free isolation solution and a Ca^{2+} containing taurine solution (Table 1) were connected to the other side of the Langendorff system separately and kept in a water bath at 38 degrees. The heart was first perfused with isolation solution for 10

minutes. Ca^{2+} free solution was used as it was shown that cells would tend to separate under this condition at the intercalated disc (Greve *et al.*, 1985). A mixture of 9.6% collagenase (Worthington, 40C20110) and 1.8% protease (Sigma, P5147) would be added to isolation solution at the end of the 10 minutes period at the ventricle will be continued to be perfused with this solution mixture. Enzymes were added to facilitate cell separation as they will digest the extracellular matrix. The surface of the heart would be carefully monitored from this stage. As the digestion progresses, the heart will start to exude mucus-like fluid. At first, the surface would appear to be sweaty and can be easily wiped clean with hand. The fluid would gradually become sticky and form a 'gloop' between the heart and glove when trying to wipe it (Fig.11). Once the 'gloop' became thick and can reach 2cm long, the perfusion solution would be switched to taurine solution and left for further 20 minutes. Introducing of taurine into the Ca^{2+} free solution is known to have protective effect to myocyte and help them regain the tolerance to Ca^{2+}(Isenberg and Klockner, 1982). The well-digested part of the left ventricle would show a colour change from pink to brown, this part would be cut-off from the heart, cut into small pieces and agitated in taurine solution. Isolated left ventricular myocytes should fall apart in the solution, and the solution was filtered (200 µm mesh) into falcon tubes to remove chunks of tissue. Tubes were rested for the myocytes to form a pallet, then the supernatant would be removed, the cells would be resuspended in 1:1 taurine and normal tyrodes solution mixture to avoid cell death from sudden exposure to high Ca^{2+} concentration.

	Isolation solution (pH to 7.34)	**Taurine solution (pH to 7.34)**	**Normal tyrodes solution (pH to 7.34)**
Bovine serum albumin (BSA) (Sigma, A6023)	0.5 mg/ml	0.5 mg/ml	
2,3-Butanedione monoxime (Sigma,B0753)	10 mM	10 mM	
NaCl	134 mM	113 mM	140 mM

Hepes(Fisher,BP310)	10 mM	10 mM	10 mM
Glucose	11 mM	11 mM	10 mM
KCl(1M)	4 mM	4 mM	4 mM
$MgSO_4$(1M)	1.2 mM	1.2 mM	
NaH_2PO_4(1M)	1.2 mM	0.1 mM	
Taurine(Sigma, 86329)		50 mM	
$CaCl_2$(1M)		0.1 mM	1.8 mM
$MgCl_2$			1 mM
Probenecid (Sigma,P8761)			2 mM

Table.1 Recipe of isolation solution, taurine solution and normal tyrodes solution.

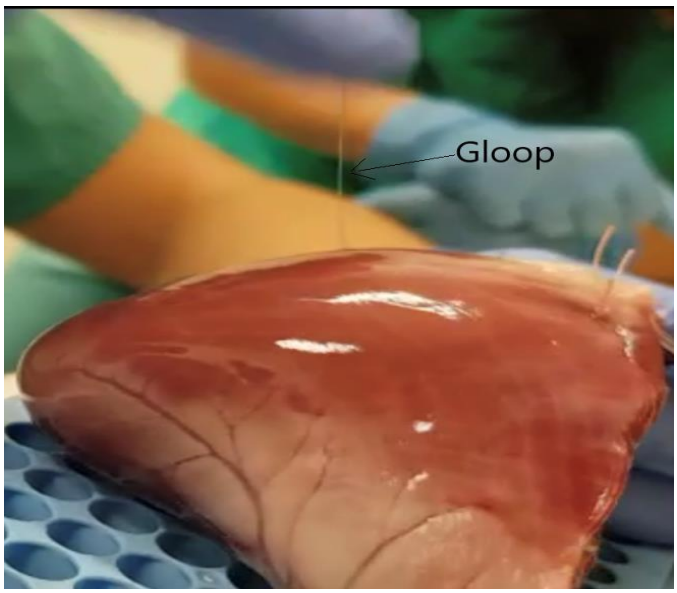

Fig.11 Example of a 'gloop' formed when the cardiac tissue is being digested by the enzymes during cell isolation.

2.6 Cell fixation

Resuspended left ventricular cells would be added to an 8-well Ibidi plate (Ibidi, 80806) at 500 µl cell suspension per well, and left to rest for 30-60 minutes for the cells to settle and adhere to the bottom of the plate. Cells were first washed once with PBS for 5 minutes, if a phosphorylation treatment is required then 200nM isoprenaline in PBS

was be used instead of PBS at this step. Isoprenaline was used as it is an analogue of adrenaline, therefore is a mixed β-adrenergic receptor agonist and would activate the catecholamine response, and the activity of proteins with phosphorylation sites, e.g. PLN, could be examined. All the liquid is then removed and replaced with 3% PFA in PBS and the cells were fixed for 10 minutes, then washed for 3 times for 5 minutes (Fig.12). Fixed cells would be stored at 4°C and used for STORM imaging within a week.

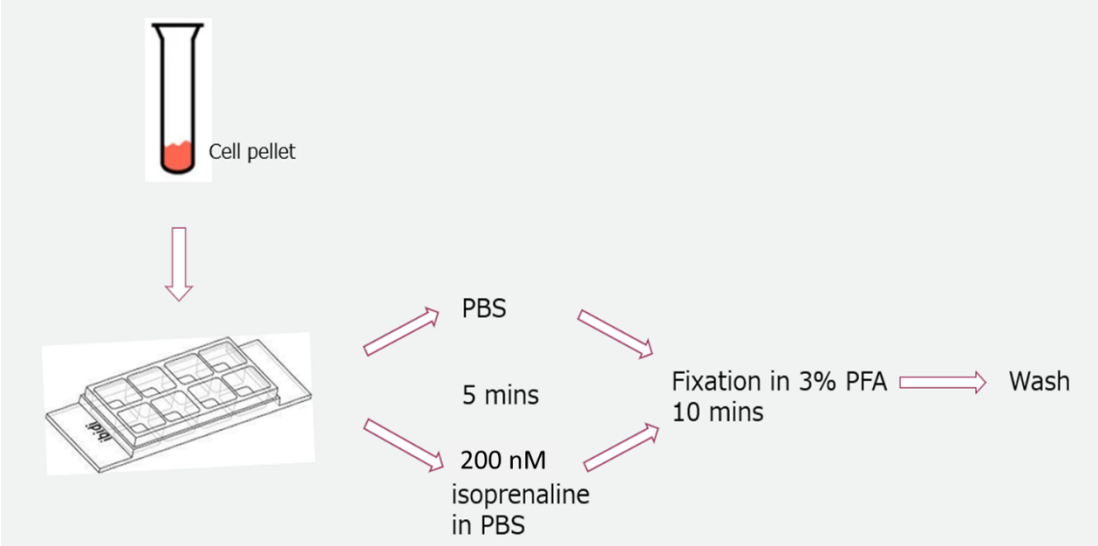

Fig.12 Flow chart of cell fixation process.

2.7 Protein extraction

Ventricular tissue samples were collected from fresh sheep hearts and immediately conserved in liquid nitrogen. For the myocardial infarction sheep model, tissue samples were collected for two specific areas: the border zone which is within 1cm of visible boundaries of the infarction; and the remote zone which is at least 2 cm away from the infarction. Lysing buffer was prepared before each protein extraction and contained 1% protease and phosphatase inhibitor complex (PPIC) (Sigma, PPC1010) in the radioimmunoprecipitation assay buffer (RIPA) buffer (Sigma, R0278). The presence of protease and phosphatase inhibitors was to stop any de-phosphorylation to maximize the retention of the original protein phosphorylation state in live animals. Approximately 100 mg of desired tissue was put into a homogenizer tube with beads and added with 1 ml (1:10 w/v) of the lysing buffer. Tissues were homogenized in Precellys® Evolution homogenizer (Bertin Technologies) at 7200 rpm for 3 times 30 seconds and then centrifuged at 10000 g, 4°C for 10 minutes to sediment the insoluble

fraction. The supernatant which contained solubilised proteins was then aliquoted and stored and – 80 °C until use. For protein extraction from cells, 1 tube of isolated cells would be used instead of the tissue. Cells would be washed in normal tyrodes solution (or 1% isoprenaline in NT if isoprenaline treatment is required) for 5 minutes, then replaced with lysing buffer and homogenized at 6000 rpm, 4°C for 2 times 30 seconds.

2.8 Protein concentration quantification

Protein concentration was determined using a Bradford detergent compatible colorimetric assay. Extracted protein was first diluted by 1 in 10 in RIPA buffer (Sigma, R0278). 5µl RIPA buffer (using as the blank), 7 BSA standards (Thermo scientific, 23208) and protein dilutions were then sequentially added into a 96-well plate, all in triplicates. The Bradford reagent A (Bio-rad, 5000113) was mixed with reagent S (Bio-rad,5000115) in a 50:1 ratio and 25 µl of the mixture was added to each well. Finally, 200µl Bradford reagent B (Bio-rad, 5000114) was added to each well and left for ~15minutes for the reagent to react with protein. The plate was read with a Synergy HTX multi-mode reader (Bio-Tek) and excited at 595nm, and the absorbance of the blank and BSA standards was used to plot a standard curve (Fig.13). The standard curve was used to calculate the diluted protein concentrations and multiplied by 10 to give the original protein concentrations.

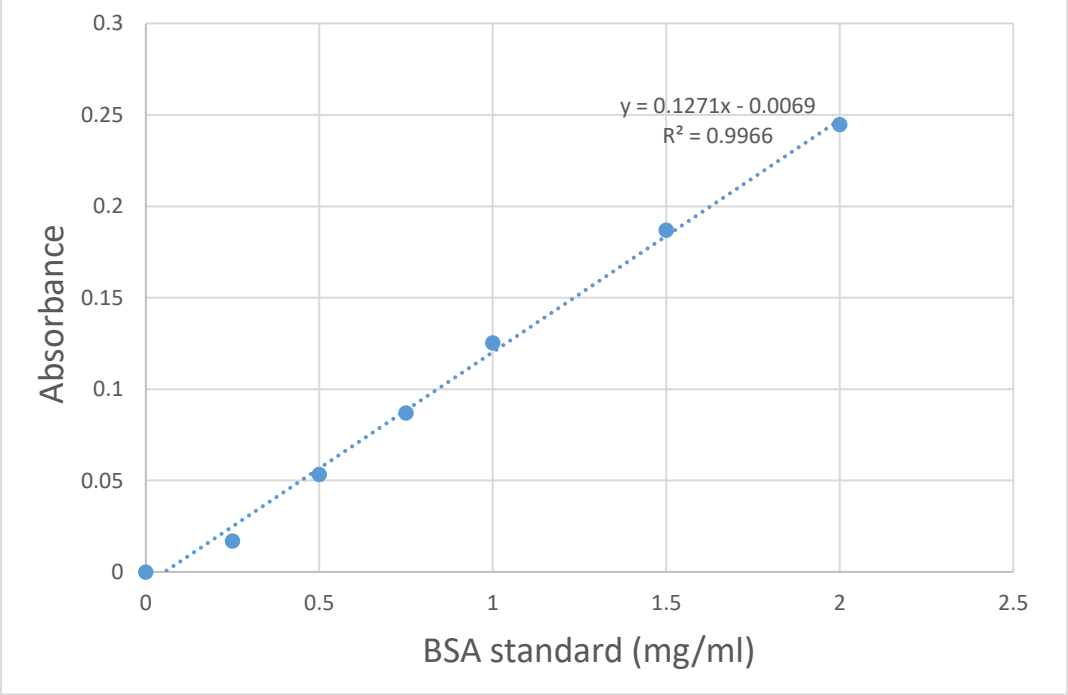

Fig.13 An example of a BSA standard curve.

2.9 Western blot

Each sample lysate was prepared with 5 µl Sample Buffer (Invitrogen, 2083421), 10 µg protein (volume depending on the protein concentration), 10% v/v NuPAGE Sample Reducing Agent 10X (Novex, NP0004) and made up to 20 µl with RIPA buffer (Sigma, R0278). Samples were heated in a heat block at 95°C for 3 minutes to denature the protein. 18.5µl of each protein lysate was loaded into the wells of a NuPAGE 4 -12 % bis-tris gradient gel (Invitrogen, 21020411) along with one well of 7 µl molecular weight ladder (Bio-rad, 1610375). The gel was run in a gel tank filled with Running buffer prepared with 950 ml Mili Q water and 50ml 20X NuPAGE Running buffer (type depending on protein size, see table), then transferred with membrane transfer buffer prepared with 750 ml Mili Q water, 20% methanol and 50ml 20X NuPAGE transfer buffer (Novex, NP0006-1). Running and transferring time were assay dependent and determined by the molecular mass of the protein of interest (see Table.2). The transferred membrane was blocked with either 1% skimmed milk in TBST or Sea Block (for phosphorylated protein) (Thermo Scientific, 37527) for 1 hour. The membrane was then stained with total protein stain (Li-COR, 926-11011) for 5 minutes, imaged on the Odyssey® CLx Infrared Imaging System (Li-COR) in the 700nm channel, and then incubated with primary antibody (for specific details see Table.2) in TBST at 4 °C overnight. The next day, the membrane was washed in TBST for 3 times 5 minutes, incubated with secondary antibody diluted in TBST at 1:20,000 at room temperature in dark for 1 hour (Table.3), then washed in TBST for 3 times 5 minutes and scanned with the Odyssey® CLx Infrared Imaging System (Li-COR) in 800nm channel.

Protein	size	Running buffer, running time and voltage	Transfer time and voltage	Primary antibody and concentration	Secondary antibody
SERCA	100 kDa	MOPS running buffer (Novex, NP0001) 200V 1 hour	30V 75mins	SERCAA2 mouse monoclonal (Santa Cruz,sc-73022) 1:3000	IRDye 800CW Goat anti-mouse IgG (H+L) (Li-COR, 925-32210)
PLN	5 kDa	MES running buffer (Novex,NP0002) 50V for 20mins then 170V for 55 mins	30V 75mins	Phospholamban mouse monoclonal (Invitrogen, MA3-922) 1:5000	IRDye 800CW Goat anti-mouse IgG (H+L) (Li-COR, 925-32210)

pPLN	5 kDa	MES running buffer (Novex,NP0002) 50V for 20mins then 170V for 55 mins	30V 75mins	Phospholamban pSer16 rabbit polyclonal (Badrilla, A010-12) 1:2500	IRDye 800CW Goat anti-rabbit IgG (H+L) (Li-COR, 925-32211)

Table.2 Conditions, antibodies and concentrations used for each protein in western blot.

2.10 Western blot analysis

Image studio (LiCor, UK) was used to analyse Western blot images. A region of interest (ROI) was drawn on the total protein image around where the desired protein band was located for each lane to quantify the signal. Each ROI should only include one lane of protein and should be including the same length of the protein band (Fig.14). The signal of each lane was divided by the signal of the lane with the highest intensity to give a lane normalization factor. Then the signal quantification step was repeated with the target protein bands on the 800 nm image. The target band signal of each lane was divided with the lane normalization factor worked out in the previous step to give a final normalized signal.

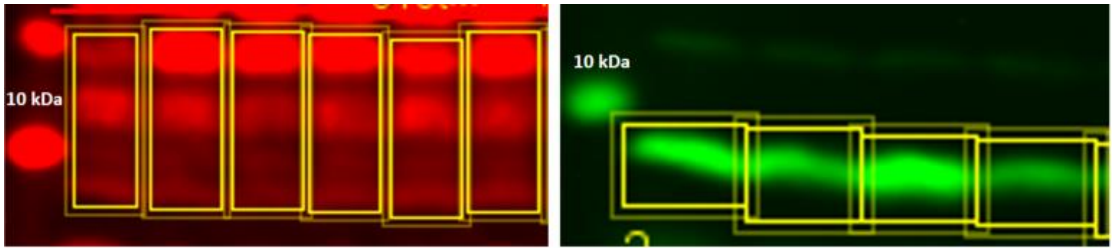

Fig.14 Example of the how the area is selected for total protein and target protein analysis. On the left-hand side, total protein area is selected around the targeted protein located (where in this sample is around 10 kDa) and the ROI is drawn at the same length for each lane; on the right-hand side, ROI is drawn around the targeted protein at the same size.

2.11 Immunofluorescence labelling

Fixed cells were first washed once with PBS, then permeabilized with 0.25 % Triton for 30 minutes to break through the cell membrane thus allowing antibody penetration to the intracellular compartment. Cells were then washed once with PBS and incubated with an image enhancer (Invitrogen, I36933) for another 30 minutes. Image enhancer helps reducing the non-specific binding of off-target proteins and helps lower background signal from non-specifically bound fluorescent probes. Cells were then washed for 3 times 5 minutes and blocked with 0.05 % Triton, 10 % natural goat serum

and 5 % glycine in PBS for 90 minutes to reduce non-specific binding of antibodies on the background. Blocking solution was then replaced with primary antibody (Table.3) with 0.05 % Triton, 5 % natural goat serum in PBS and incubated overnight at 4 °C. The next day, cells were washed with 0.05 % Triton, 10 % natural goat serum in PBS for 3 times 10 minutes and incubated with secondary antibody (Table.3) in 0.05 % Triton, 5 % natural goat serum in PBS in dark for 1 hour at room temperature. Cells were washed again with 0.05 % Triton, 10 % natural goat serum in PBS for 3 times 10 minutes. Cells were then post-fixed with 3 % PFA for 10 minutes. If two primary antibodies were required, the second primary antibody was conjugated with a Zenon labelling kit prior to use and incubated before the fixing step.

The Zenon labelling protocol consists of incubating fluorophore labelled Fab fragment with the primary antibody following with addition of non-specific IgG to block the unbound Fab fragment This kit allows primary antibodies originating from the same species to be used together. Here, 2 µl primary antibody was added to 8 µl PBS and incubated with 5 µl Zenon labelling solution for 5 minutes. 5 µl Zenon blocking solution was then added to block any unbound Zenon antibody. The solution was then made up to 100 µl with 0.05 % Triton and 0.05 % natural goat serum in PBS, which gave a final primary antibody concentration of 1 in 50. Zenon conjugated primary antibody was then added to the cells previous to the fixing step and incubated for 1 hour at room temperature and washed once with PBS before fixing.

Combination	First Primary antibody and concentration	First secondary antibody	Second primary antibody	Second Zenon secondary antibody
SERCA+PLN	SERCA2a mouse monoclonal(Santa Cruz,sc-73022) 1in100	Alexa fluor Goat anti-mouse IgG (H+L) 647 (Invitrogen, A-21235) 1in500	Phospholamban mouse monoclonal (Invitrogen, MA3-922)	Zenon Mouse IgG2a 488 Labelling Kit (Invitrogen, Z25102)
SERCA+α-actinin	α-actinin mouse monoclonal (abcam,ab9465) 0.7in100	Alexa fluor Goat anti-mouse IgG (H+L) 488 (Invitrogen, A-11001)	SERCA2a mouse monoclonal(Santa Cruz,sc-73022)	Zenon Mouse IgG1 647 Labelling Kit (Invitrogen, Z25008)

		1in500		
PLN+α-actinin	α-actinin mouse monoclonal (abcam,ab9465) 0.7in100	Alexa fluor Goat anti-mouse IgG (H+L) 647 (Invitrogen, A-21235) 1in500	Phospholamban mouse monoclonal (Invitrogen, MA3-922)	Zenon Mouse IgG2a 488 Labelling Kit (Invitrogen, Z25102)

Table.3 Combination of primary antibodies and secondary antibodies systems used in immunoflurosent staining.

2.12 STORM imaging

Cells were always be stained one day prior to imaging. Before imaging, the solution in the well was replaced with a switching buffer contained catalase (1 μg/ml) (Sigma, C100), glucose oxidase (50 μg/ml) (Sigma, G2133) and cysteamine hydrochloride (100mM) (Sigma, M6500). The enzymes and cysteamine hydrochloride acted as oxidation and reducing agents that would switch the fluorophores on and off resulting in the fluorescent labels on the cells 'blinking'(Nahidiazar *et al.*, 2016). Cells were imaged under a Nikon microscope with the Nis-Element STORM programme. Each run of the STORM imaging would take 10,000 images per channel that would record the randomly activated 'blinks' every ~ 10 ms and reconstructed them together to give the final image. Cells were picked randomly from the plate and images were focused in the middle of the cell avoiding nuclei at a single layer with the facilitation of TIRF(see section 1.5.3), and the typical TIRF angle is between 60° - 62°. 5 cells were imaged per treatment per sheep (i.e. control or isoprenaline treated).

2.13 STORM imaging analysis

STORM images were first analysed with Nikon NIS-Elements v4. Thirty random blinks were selected per channel per cell and the intensities of them were measured. A 90th centile value of the 30 blinks' intensities was calculated and this value was set as a threshold to filter out background noise. These analysed STORM files were used for two further analyses: proximity analysis that demonstrate the proximity of protein clusters from two channels, i.e. the distance between two different proteins; and cluster analysis that gave the parameters of protein clusters within a single channel. For proximity analysis, STORM files were imported into a custom written MATLAB

routines would automatically calculate the minimum, median, maximum, and mean distance in nm between proteins from two channels. The mean distance was taken, and the average was calculated from the 5 cells from the same treatment in the same sheep. For cluster analysis, each channel in a STORM file was imported separately to a programme called Cluster written by Prof Andrew Trafford. 10 regions on the myocyte Z line were randomly picked in one cell and the programme would measure the average protein cluster sizes, the distance between the centres of one cluster and its nearest cluster and the distance from the edge of one cluster to its nearest cluster (Fig.15). An average was taken for each of these three parameters from the 10 regions to give the parameters for one cell, and the results of 5 cells from the same treatment in the same sheep were averaged again to give the final value.

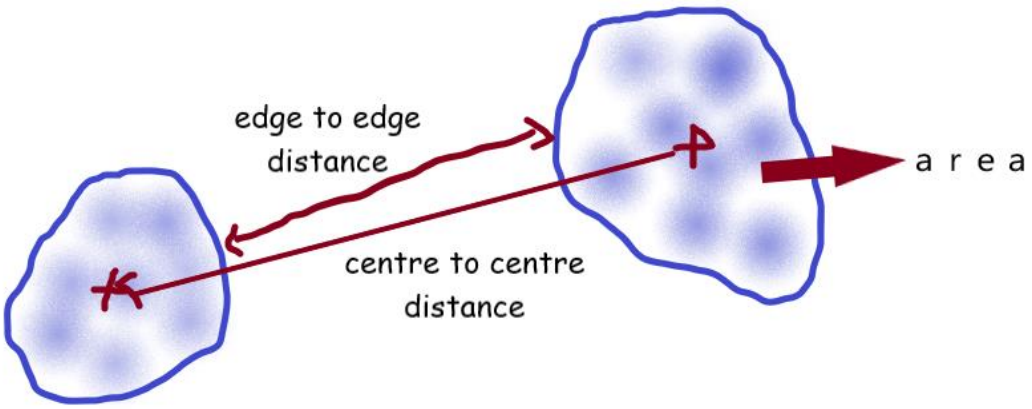

Fig.15 An illustration of how data of clusters characteristics were taken, in which the two groups of blue dots circled with solid line indicate two clusters.

2.14 Statistical analysis

Data are expressed as mean ± standard error of the mean (S.E.M), n cells from N animals. Statistical analysis was performed with GraphPad Prism version 8.01 (GraphPad Software, USA). Normal distribution was evaluated using the Shapiro-Wilk test. 2-sided paired Student t test was used for PPIC confirmation experiment. Ordinary two-way ANOVA was used to test multiple comparisons. For the nonnormally distributed data or the data with small a number (<6) to determine normality, the Mann-Whitney U test was used for 2-group analysis, and the Kruskal-Wallis test with post hoc Dunn multiple comparisons test was used for >2-group analysis. $P<0.05$ was used to define statistical significance.

Chapter 3

Results

3. Results

3.1 Confirmation of phosphorylation maintenance in protein extraction

Protease and phosphatase inhibitor cocktail was added to all protein extraction steps to maintain the original phosphorylation state believed to be present in animals. To confirm the efficacy of the cocktail, isolated ventricular myocytes were first treated with 200nM isoprenaline, then protein was extracted with or without the inclusion of a protein phosphatase inhibitor cocktail (PPIC) and samples blotted for pPLN to compare the phosphorylation level of PLN (Ser16) and thus efficacy of the PPIC in maintaining protein phosphorylation status (Fig.16). It could be seen that samples added with PPIC had successfully preserved the phosphorylation state.

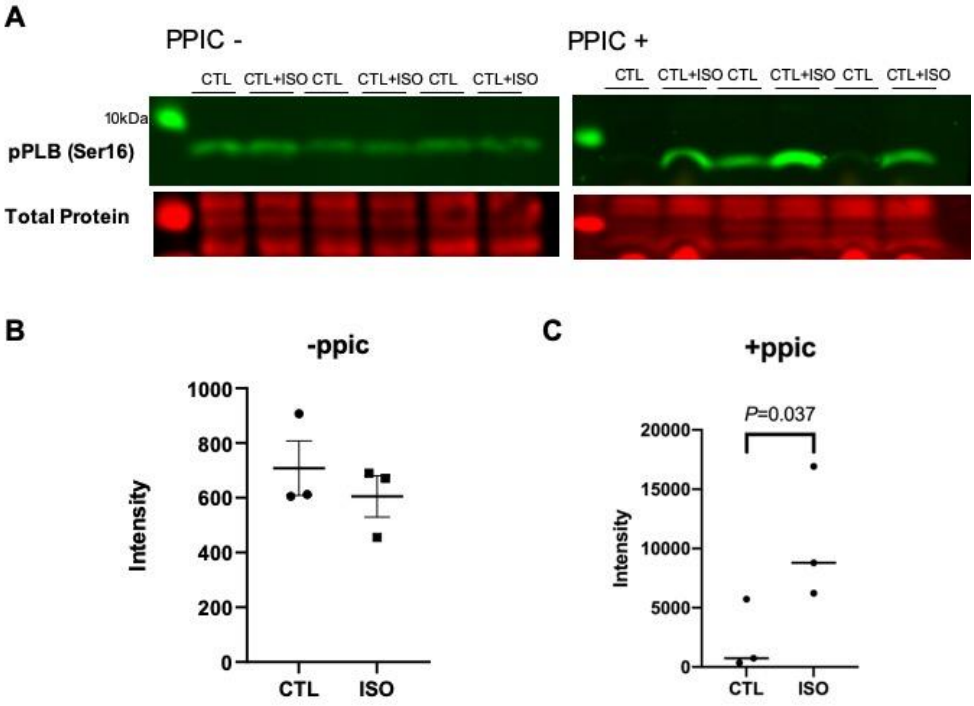

Fig.16 Ser16 pPLN abundance in freshly isolated control sheep ventricle cells. (A) Original copy of the western blot. (B) Before adding with PPIC, there was no difference in the pPLN abundance between control and isoprenaline treated cells. (C) After adding with PPIC, there is more pPLN in isoprenaline treated cells indicating the cells were successfully phosphorylated and de-phosphorylation was prevented. N = 3 biological repeats

3.2 verification of animal model

In vivo data of MI and control animals were generated by Dr Barbara Niort. After allowing the animal to recover from surgical procedures their cardiac function was monitored every week using multiple clinical parameters including echocardiography. Twenty weeks following the surgery, we observed a significant reduction in systolic ejection fraction of more than 40% (Fig.17), as well as an increase in left atria antero-posterior dimensions. The incidence of ventricular arrhythmia 72 hours post-myocardial infarction, which is associated with increased in hospital mortality, was also monitored. We observed the presence of ventricular ectopic activity in 83 % of the animals, as well as ventricular tachycardia/ fibrillation in 17% of animals. At the end of the 20 weeks, the animals were euthanised. After heart extraction apicoseptal transmural necrosis involving all 3 layers of the heart was clearly visible (Fig.18).

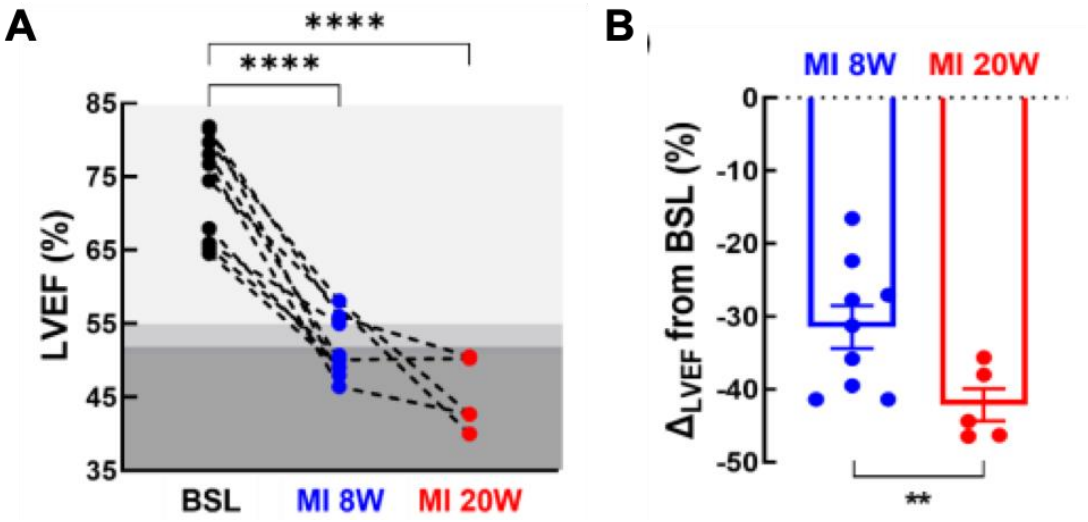

Fig.17 Reduction of ejection fraction in MI sheep model.

LVEF: left ventricle ejection fraction, BSL: baseline

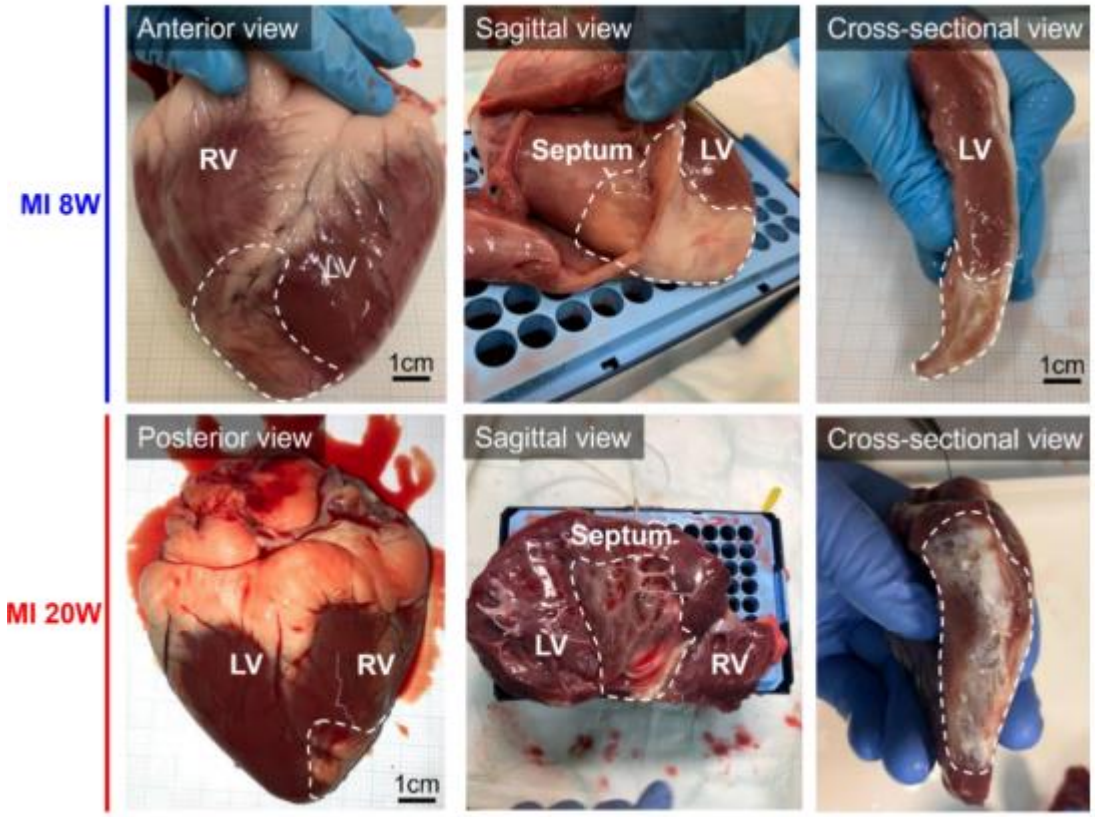

Fig.18 Representative images of infarction formed in 8W and 20W post-MI sheep. Infarcted areas are circled with dashed white lines. Pictures were obtained from Dr Barbara Niort.

3.3 Protein abundance

The expression/abundance changes of Ca^{2+} handling proteins, e.g. SERCA and PLN, are inconsistently reported in the literature (see section 1.3.3). Given these considerations, the first series of experiments that I performed were to determine how key Ca^{2+} regulatory protein abundance altered in the 20 week post MI sheep model that we have developed in this laboratory. As such I had determined the protein abundance of SERCA, PLN, and the active form pPLN in the border and remote regions of the left ventricle in our ovine MI model and compared these to control animals using western blot.

3.3.1 SERCA abundance was increased in MI sheep

SERCA abundance was found to have a 33.8 ± 10 % increase in 20W MI sheep ventricle remote zone in comparison to the control ventricle (P = 0.0374). Increasing trend was also seen in the 20W border zone (25.6 ± 9%), however was not significant

(P = 0.065). There was no difference in SERCA abundance between the control, 8W MI border zone and remote zone (all P > 0.9999) (Fig.19).

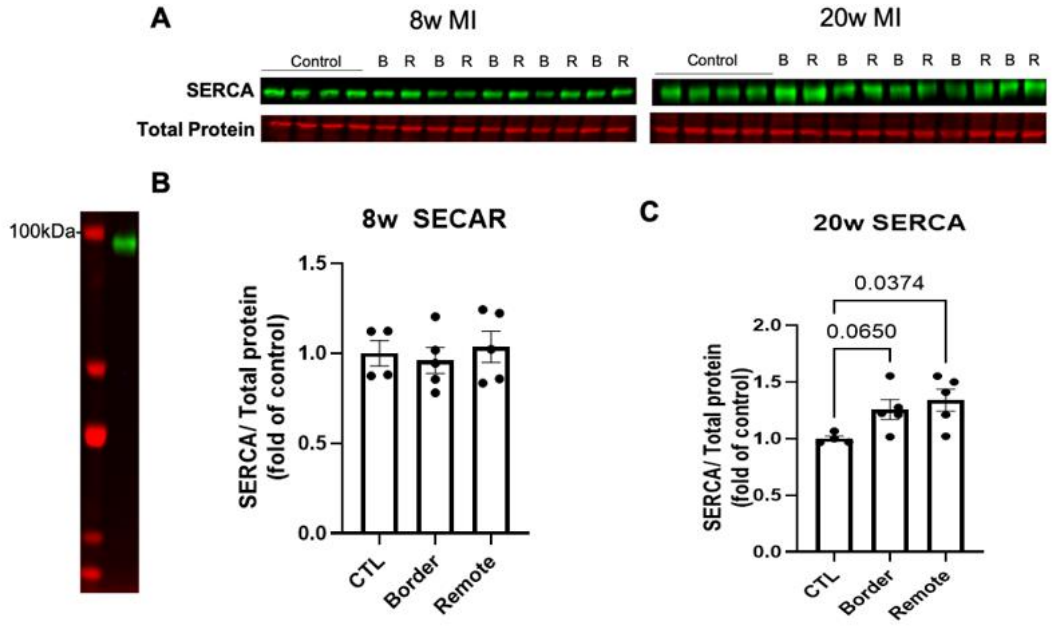

Fig.19 SERCA abundance in control, 8W and 20W MI sheep ventricle. (A) Original copy of SERCA Western blot. (B) SERCA protein abundance in control, 8W border and 8W remote zone. There is no difference between the three groups. (C) SERCA protein abundance in control, 20W border and 20W remote zone. SERCA abundance increased from control to 20W MI, specifically there is higher abundance in the remote area. N=4 biological replicates in CTL and 5 in MI.

TP: total protein, CTL: control, B: border, R: remote

3.3.2 PLN abundance remained unchanged in 8W and 20W MI sheep

There is a decreasing trend of PLN abundance from control to 20W MI sheep ventricle border zone (16.3 ± 9% decrease, P =0.785) and remote zone (22.87 ± 9% decrease, P = 0.1019), however, analysis revealed no statistical difference. Similarly, no significant difference was found between the ventricle of control, 8W MI border and remote zone (CTL vs border, p>0.9999; CTL vs remote, P = 0.2827) (Fig.20).

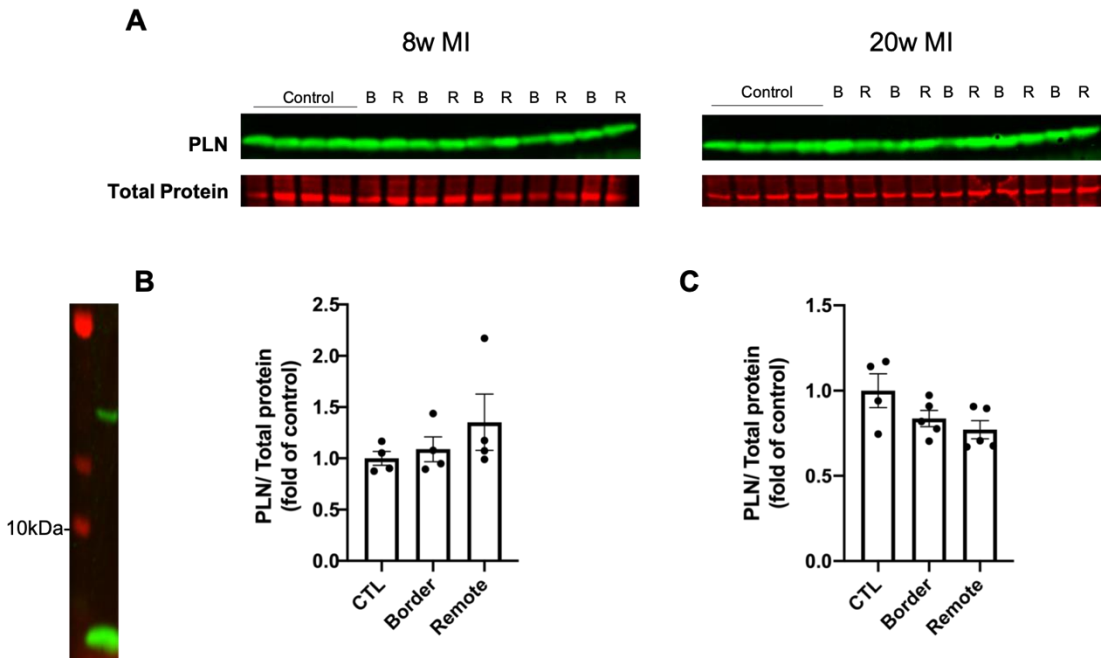

Fig.20 PLN abundance in control, 8W and 20W MI sheep ventricle. (A) Original copy of PLN western blot. (b)PLN protein abundance in control, 8W border and 8W remote zone. There is no change from CTL to 8W border and remote area. (c) PLN protein expression in control, 20W border and 20W remote zone. There is a decreasing trend in PLN abundance from CTL to 20W MI. N=4 biological replicates in CTL and 5 in MI.

TP: total protein, CTL: control, B: border, R: remote

3.3.3 pPLN abundance was slightly decreased in MI sheep

pPLN had shown a decreasing trend in both 8W and 20W MI in comparison to control sheep ventricle, however, none of these changes is significant according to the statistical analysis. The reduction in 20W MI sheep is larger than in 8W. In 8W MI, pPLN in the border zone had a decrease of 37 ± 30% than control (P = 0.2176), and in the remote zone there was a 50 ± 17% decrease (P = 0.3292). In 20W MI, the reduction was 48 ± 25% from control to the border zone (P = 0.2338) and 65 ± 12% to the remote zone (P = 0.1086) (Fig.21).

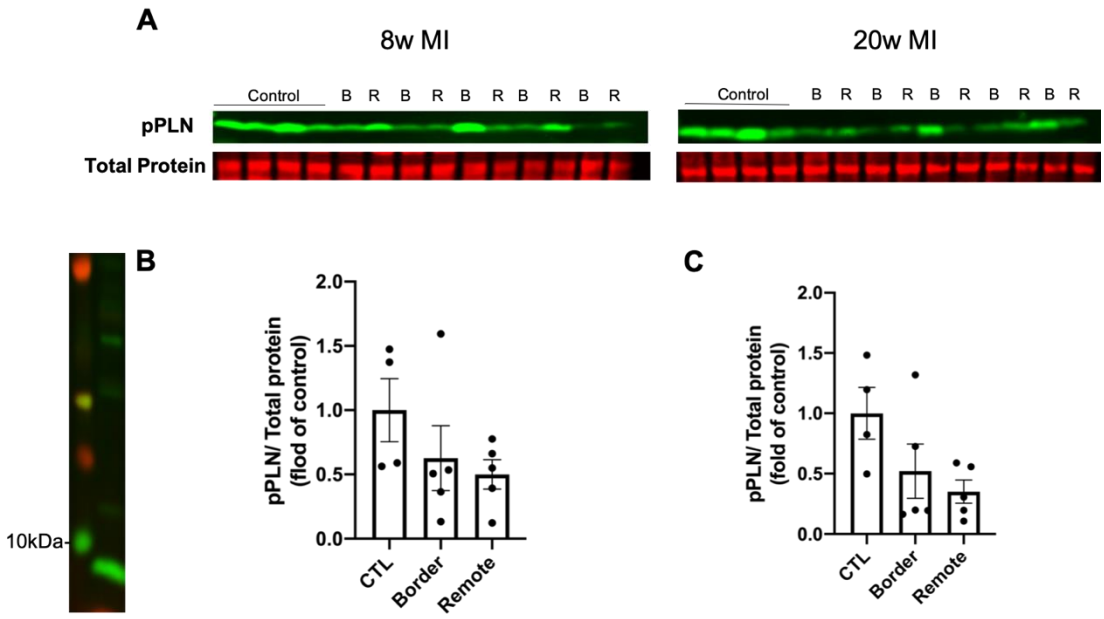

Fig.21 pPLN abundance in control, 8W and 20W MI sheep ventricle. (A) Original copy of Ser16 pPLN western blot. (B) Ser16 pPLN protein abundant in control, 8W border and 8W remote zone. There is no difference between the three groups. (C) Ser16 pPLN protein abundance in control, 20W border and 20W remote zone. pPLN abundance had no difference from control to 20W MI border and remote zone but showed a gradually decreasing trend. N=4 biological repeats in CTL and 5 in MI.

TP: total protein, CTL: control, B: border, R: remote

3.4 STORM imaging

Whilst no statistical difference was noted in the abundance of some key Ca^{2+} regulatory proteins by Western blotting it remains possible, based on emerging data focusing on the RyRs (see section1.5), that the spatial distribution of these proteins is perturbed and that this then may underlie alterations to contractility or arrhythmia susceptibility. To this end Ca^{2+} sparks frequency and amplitude was found to be related with RyRs cluster size, and optimal size is required to create responsible sparks for maintaining cardiac contraction without triggering arrythmia. Importantly, no such characterization of the subcellular distribution of SERCA and PLN has thus far been reported. Additionally, whether catecholamine stimulation and thus phosphorylation of PLN impacts on the nanoscale distribution of SERCA and PLN and their proximity to one another is currently unknown. Therefore, the next series of experiments were designed to evaluate the nanoscale distribution of SERCA and PLN in ventricular myocytes and to determine how this distribution and the spatial proximity between SERCA and PLN is altered in

in response to catecholamine stimulation. To achieve these objectives, STORM imaging was performed on isolated ventricular myocytes and in response the treatment with isoprenaline.

3.4.1 Cluster distance is smaller in PLN after phosphorylation but not different in SERCA

200nM isoprenaline was applied to control sheep cardiac ventricular myocytes to promote catecholamine dependent phosphorylation of PLN. Following isoprenaline treatment there was shorter distance between PLN clusters both from assessed using the centre to centre (791.9 ± 13.31nm and 525.6 ± 22.2nm, mean ± SEM) and edge to edge distances (823.5 ± 33.8nm and 581.1 ± 31.8nm) (all *P* value < 0.0001). Conversely, isoprenaline treatment had no effect on the centroid to centroid or edge to edge distance between SERCA clusters (773.7 ± 22.8 and 788.1 ± 26, centre to centre; 429.3 ± 28.6 and 439.1 ± 8, edge to edge) (Fig.22,23).

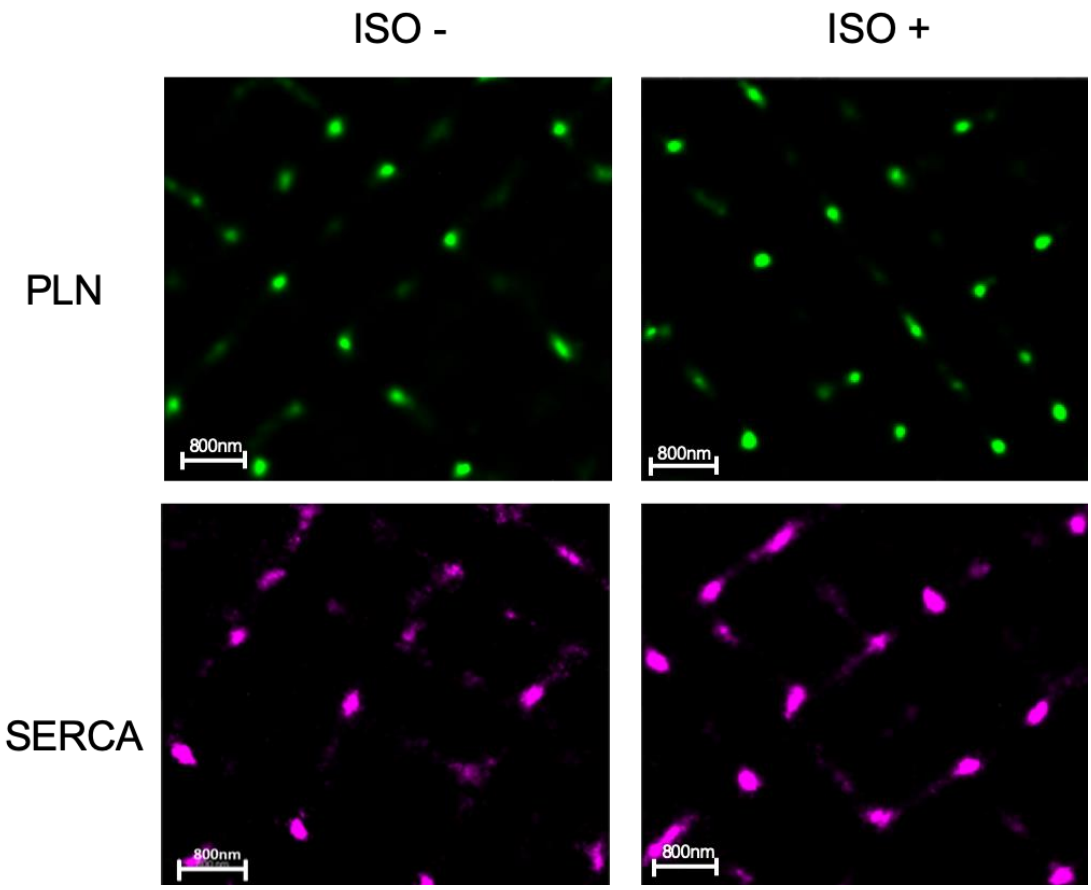

Fig.22 Sample STORM image of PLN and SERCA distribution in baseline and isoprenaline treated control sheep ventricle cells under the same scale.

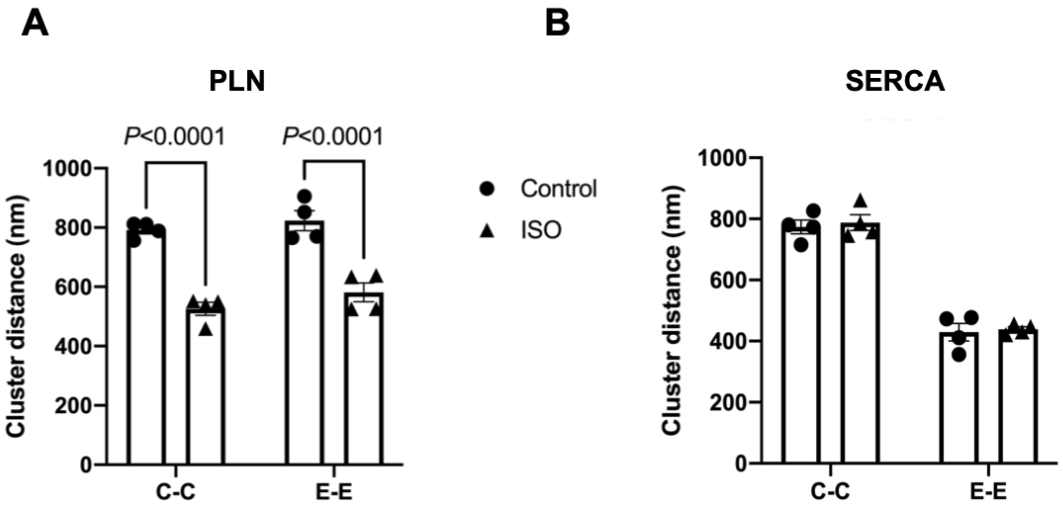

Fig.23 Mean distance between clusters within (A) PLN and (B)SERCA protein in baseline and isoprenaline treated control ventricle cells. (A) PLN centre to centre and edge to edge distance is reduced after isoprenaline treatment. (B) No change is found in SERCA clusters C-C and E-E distance before and after isoprenaline treatment. N=4 biological repeats for all groups, each point represents mean of 3-5 cells.
CTL: Control, iso: isoprenaline, C-C: Centre to centre, E-E: Edge to Edge.

3.4.2 Cluster area is not different in SERCA and PLN after phosphorylation

PLN clusters form non-significant smaller areas after phosphorylation by isoprenaline (control: 33654 ± 2976nm^2, iso: 28234 ± 2154nm^2, mean ± SEM) (P = 0.3429), while no different is seen in SERCA (65595 ± 17100 nm^2 and 56851 ± 6707 nm^2) (P = 0.8857). (Fig.22,24).

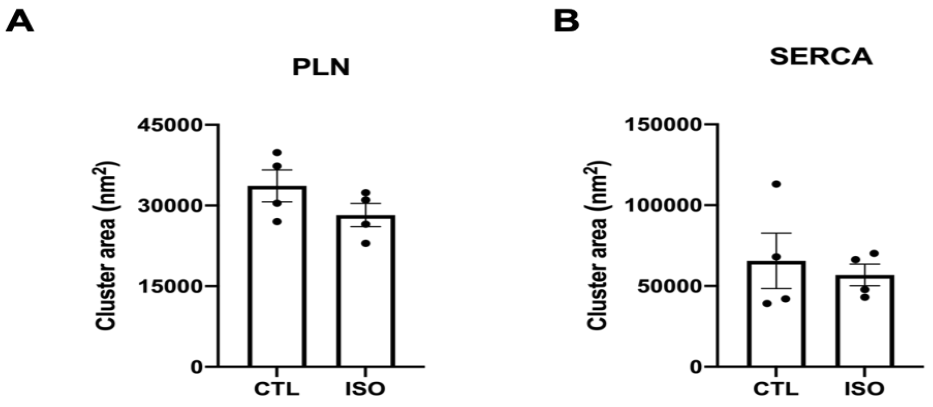

Fig.24 Mean cluster area of (A) PLN and (B) SERCA in baseline and isoprenaline treated control ventricle cells. (A) PLN cluster size is decreased after phosphorylation. (B) SERCA cluster size is unchanged before and after phosphorylation. N=4 biological repeats for all groups, each point represents mean of 3-5 cells.
CTL: Control, ISO: Isoprenaline

4.3.3 Proximity between PLN and SERCA by catecholamine induced phosphorylation

The distribution relationship between PLN and SERCA was studied with proximity analysis before and after phosphorylation in control sheep ventricular cells. Firstly, it can be seen that the SERCA to PLN distance is larger than PLN to SERCA distance, indicating that PLN proteins are always paired up with or located near a SERCA protein, while some SERCA may distribute individually without PLN association. This relationship remains unaffected after phosphorylation as neither the SERCA-PLN nor the PLN-SERCA distance is significantly different after isoprenaline treatment (both *P* value > 0.9999)(CTL: SERCA, 92.4 ± 23 nm and PLN, 45 ± 8 nm, ISO: SERCA, 83.5 ± 9.4 nm and 51.2 ± 6 nm). (Fig.25,26).

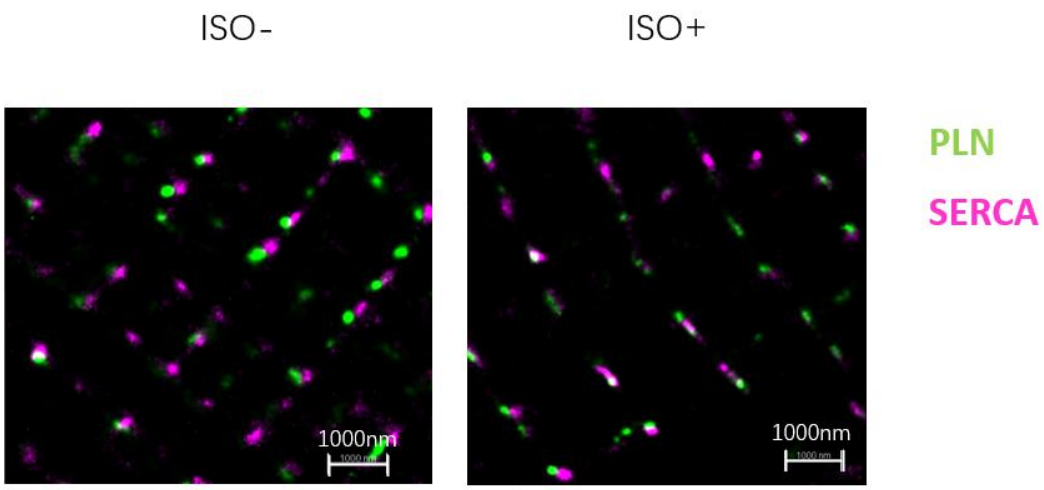

Fig.25 Sample STORM images of PLN and SERCA colocalization in baseline and isoprenaline treated control sheep ventricle cells under the same scale.

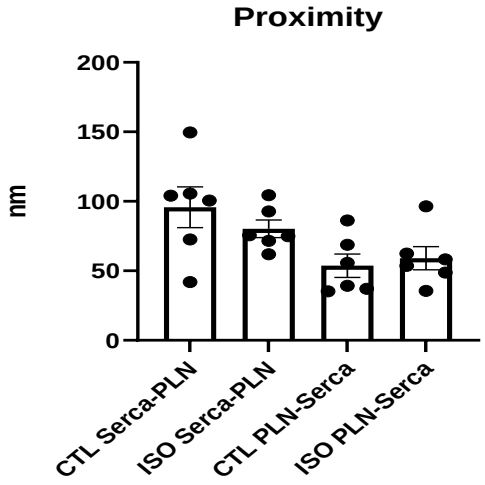

Fig.26 The proximity from SERCA to PLN and from PLN to SERCA under baseline and isoprenaline treatment conditions in control sheep ventricle myocytes. Isoprenaline treatment does not change the SERCA-PLN and PLN-SERCA distance. N= 6 biological repeats, each point represents mean of 3-5 cells.
CTL: Control, ISO: Isoprenaline

Chapter 4

Discussion

4. Discussion

Deregulation of calcium homeostasis in cardiomyocytes has been implicated in the development of heart failure. Studies have shown that the expression and activity of SERCA and PLN are altered in samples from heart failure patients. In the present thesis, I aimed to characterise changes in protein abundance and the sub-cellular distribution of SERCA and PLN in infarcted heart using a sheep MI model 8 weeks and 20 weeks post MI and compared these findings to those obtained in normal healthy sheep. I further characterised the phosphorylation status of PLN at the Serine 16 residue induced by catecholamine stimulation and whether this then led to a change in association with SERCA. Unfortunately, I was unable to complete the distribution study in the MI model as tissues were not available due to Covid mediated interruptions to animal awork at The University of Manchester. Nevertheless, the key findings of this thesis are: (1) SERCA protein abundance was significantly increased at 20 weeks post-MI in the remote area compared with the control group. (2) There was no change in PLN protein abundance between MI groups and control group, but pPLN abundance level was slightly reduced in MI groups relative to the control. (3) The distance between PLN clusters become smaller after catecholamine (isoprenaline) induced phosphorylation which may indicate an effect due to phospholamban pentamerization. (4) The isoprenaline-induced phosphorylation did not alter the cluster size or distance of SERCA. These results highlight the significance of changes in pPLN to the pathogenesis of heart failure. Moreover, they can partly explain why SERCA gene therapy has not been effective in clinical trials. Data for sub-cellular distribution of SERCA and PLN in MI was not able to be achieved due to lack of animal model.

4.1 Subcellular SERCA localization and abundance in heart failure

Using a sheep model of ischaemia reperfusion MI, I found that SERCA protein abundance gradually increased over time post-MI. This was contrary to my hypothesis. Moreover, it was inconsistent with findings from clinical samples or animal models where the mRNA expression or protein abundance of SERCA was found to be decreased or remained unchanged in heart failure. For instance, the study by Meyer et al. reported that the SERCA expression in heart failure was downregulated. This departure from previous studies may be explained by two hypotheses. (1) It is likely the MI model established in this study reflects early-stage heart failure. According to

the ejection fraction data of our sheep model, they fit more into the HFmrEF range with a trend of falling into HFrEF, which means the disease was still developing, while most clinical trials and research previously were done on HFrEF or even end-stage animals and patients. In this case, SERCA expression had not reached the threshold of decreasing as seen in terminal heart failure, and therefore may not be directly comparable to the current literature at more advanced stages of the disease. (2) Further to this, it is possible that being a model of early-stage heart failure, the infarct was still localized at the site of injury with little spreading to other parts. In such a scenario, the expression of SERCA in parts further from the infarct site may compensate for the loss of its expression at the infarct zone. However, a previous study showed that SERCA expression in patients with mild heart failure decreased slightly at mRNA level suggesting that it is unlikely to be upregulated in early stage heart failure (De Boer *et al.*, 2001). Although this weakens the above argument that the observed increase in SERCA expression is due to the likely early-stage of the heart failure model in the present study, it worth mentioning that the study was conducted on patients diagnosed with idiopathic dilated cardiomyopathy which might not be comparable with our MI model. Moreover, I detected SERCA abundance at protein level whereas they quantified its expression discussed above was at the mRNA level. This may underlie the discrepant results given that changes at mRNA levels may not be linear with changes in protein expression (Maier, Güell and Serrano, 2009). It is very important to investigate the SERCA expression/abundance in a less advanced heart failure situation and as these stages likely represent better therapeutic windows than end or late-stage disease settings. Additionally, the data for HFmrEF is still scarce and patients that are categorized into this criterion have distinct characteristics in comparison to HFrEF and HFpEF and are lacking effective treatments. Furthermore, considering that our model is continuously deteriorating in cardiovascular function, it is possible to develop into end-stage heart failure if it were kept for longer. At such a stage it may therefore be more comparable to patients that were diagnosed with heart failure at the first time which are likely to maintain most of their heart function. It is possible that if effective treatment could be achieved at this earlier timepoint, rather than slowing down the disease progression, more patients could be prevented from end-stage heart failure.

4.2 Effect of SERCA post-translational modification in HF

The increase in SERCA protein abundance may also indicate that the activity of SERCA, rather than the abundance, is more critical to consider in heart failure. Elsewhere, it was reported that the SERCA uptake rate was decreased in heart failure, especially in ischaemic cardiomyopathy, although its protein abundance was unaltered (Sen *et al.*, 2000). Some potential explanations for the discordance between function and protein abundance include: The SERCA protein can be modified by reactive oxygen specific (ROS) via *S*-glutathionylation at cysteine 674, and this modification can decrease SERCA activity and impair myocyte relaxation in mice (Qin *et al.*, 2013). In a rabbit model of atherosclerosis, the S-glutathionylation of SERCA and vessel relaxation were reduced in samples of abdominal aorta. On the contrary, SERCA oxidation was enhanced suggesting that the decreased relaxation of vessels in the aorta of rabbits with atherosclerosis may be due to inhibition of S-glutathionylation (Adachi *et al.*, 2004). Nitric oxide, a type of ROS, is also able to modify SERCA by S-nitrosylation via thiol-reactions. ROS had been demonstrated to be related with multiple cardiac event: large production of ROS during reperfusion contribute to formation of cardiac infarction (Zhang and Shah, 2008); ROS signalling leading to hypertrophy (Santos *et al.*, 2011) and high level of ROS in heart failure patients (Tokitsu *et al.*, 2016), indicating the possible significancy of ROS modification on SERCA in heart failure. Collectively, these results demonstrate that the activity of SERCA in a failing heart is influenced by several factors. Since we did not analyse the changes in SERCA activity in this study, future studies should explore whether the SERCA activity was also altered during MI.

4.3 SERCA and PLN nanoscale distribution

The SERCA/PLN complex is the primary regulator of Ca^{2+} translocation into the SR of cardiomyocytes and is also the main mechanism of cardiac relaxation (Gustavsson *et al.*, 2013). The distance and location of SERCA in relation to PLN is therefore critical to fine-tuning this process. In the present study, my results showed that the proximity between SERCA and PLN remained unchanged before and after phosphorylation. Moreover, the distance from SERCA to PLN was larger than that from PLN to SERCA. This indicates that not all SERCA proteins are paired with PLN proteins. In a transgenic study, it was observed that the inhibitory effect of PLN on SERCA reaches a saturation point when PLN expression is increased by 2.6 fold, suggesting that only ~40% of

SERCA is controlled by PLN *in vivo* (Brittsan *et al.*, 2000). On sarcoplasmic reticulum membrane, PLN exists as a pentamer which disassembles into monomers that interact with SERCA. Various SERCA clusters parameters, including size and distribution, are not affected by isoprenaline treatment which is not surprising as it is not a direct target of β-AR signalling. In future work it would be interesting to see whether the patterns of SERCA distribution would change in heart failure and, we plan to investigate continuing the present study to assess this hypothesis when more MI animals become available.

4.4 Alterations in PLN abundance and proximity to SERCA in HF

Phospholamban is a 52-amino acid protein encodes by the *PLN* gene. This protein is localised to the sarcoplasmic reticulum (SR) membrane. Functionally, it is crucial to the regulation of calcium cycling in cardiac myocytes by reversibly inhibiting SERCA activity. When phosphorylated at Ser16 by PKA or Thr 17 by (CaMKII), the inhibitory effect of PLN on SERCA is relieved (see section 1.2.3), which enhances the SERCA mediated translocation of Ca^{2+} into the SR.

The interaction between PLN and SERCA plays an important role in cardiac myocyte contraction and relaxation, and this interaction is tightly regulated by the β-AR signalling pathway and this mechanism is critical to achieving acute regulation of cardiac function (MacLennan and Kranias, 2003b). In this study, I aimed to characterise changes in PLN protein abundance at 8 weeks and 20 weeks post-MI induction in sheep. Partially in line with our hypothesis, the protein abundance of PLN was not altered in 8W models but showed a non-statistical trend toward a decrease 20 weeks post MI. Further work with additional samples will be required to determine if the lack of difference detected here is simply because my study is underpowered. It is unlikely that technical issues such as poor blot protein transfer explain the findings as this would not be expected to specifically affect one experimental group. The non-statistical trend was consistent with results obtained in most previous studies. For example, in failing human dilated cardiomyopathy, PLN protein levels normalized per total protein were decreased by 18% in the failing myocardium, but this decrease was not statistically significant when compared with levels in non-failing myocardium when normalization was performed using the intra-SR calcium buffer calsequestrin. The study showed that the SERCA:PLN ratio was decreased in failing heart (Meyer *et al.*, 1995). However, this was not reproduced in the present experiments. This may suggest that the

phosphorylation state of PLN, rather than the SERCA: PLN ratio has a much more significant role in the pathogenesis of heart failure. More discussion on this is presented in later sections of this discussion.

Further experiments showed that the distance between PLN clusters was decreased after catecholamine-induced phosphorylation. One potential mechanism underpinning this observation is via pentamerization of PLN monomers. This observation corroborates data obtained in a previous study in which PLN phosphorylation resulted in the formation of pentamers which are not capable of inhibiting SERCA (see section1.2.3) albeit in this study, in situ measurements of the nanoscale positioning of PLN were not reported. Herein, it was also observed that the distance from PLN to SERCA was not also altered after phosphorylation, suggesting that the pentamerized PLN did not detach from SERCA. Physiologically, PLN exists in a dynamic equilibrium between monomers and homopentamers where the oligomeric state acts as a reservoir (see section 1.2.3). The finding reported here is supported by a study that examined the interaction between PLN pentamer and SERCA using 2D co-crystallization technology. They hypothesized that the pentamer can release a PLN monomer during diastole leaving a tetramer associated with SERCA and rapidly pick up the monomer when phosphorylated. In this way, the PLN pentamer serves as a reservoir of PLN monomer to meet the ECC cycle demand, and maintain the PLN-SERCA interaction (Glaves *et al.*, 2011). Another study found that the PLN pentamer can be phosphorylated by PKA and has a higher affinity to PKA compared with monomers. Therefore, PLN pentamers may delay the phosphorylation of PLN monomers and might be a mechanism for maintaining the diastole cycle in normal cardiac physiology (Wittmann, Lohse and Schmitt, 2015). The authors had postulated that cardiac myocytes lacking PLN pentamer would have a weaker ability to cope with left ventricle pressure overload, hence the loss of PLN associates with greater susceptibility to heart failure. The same study found that a pPLN monomer fully dissociated from SERCA but not the phosphorylated pentamer as determined using co-immunoprecipitation assay, which was in agreement with a previous hypothesis that monomers reassembled into pentamers after phosphorylation and remained interacted with SERCA. In future study, the distance between PLN protein clusters will be analysed using MI model to see if the oligomerization is interrupted which may contribute to the pathogenesis of heart failure. This is rational given that Ca^{2+} re-uptake process is impaired in cardiomyocytes

from animal and human failing hearts. Moreover, failing heart show decreased catecholamine responsiveness due to remodelling of β-adrenergic receptor (Woo and Xiao, 2012).

4.5 Changes in PLN phosphorylation during HF development

Phosphorylation of PLN by PKA at Ser16 or CaMKII at Thr17 removes its inhibitory effect on SERCA leading to increased cardiac contractility. In human failing myocardium, it was reported that the phosphorylation of PLN at Ser16 was decreased (Simmerman and Jones, 1998). In the present study using an MI model I hypothesized that pPLN abundance would be decreased as it is in the sheep model of heart failure developed in this laboratory (Briston *et al.*, 2011). Indeed, the results showed that although PLN abundance was not changed in the MI model of sheep, pPLN abundance exhibited a trend toward a decrease, especially at the 20W time-point in the remote MI zone. This matches with findings from other studies (Simmerman and Jones, 1998; Mishra *et al.*, 2002). However, this study could not provide a ratio of pPLN/PLN due to incomplete experiment preparation, as no internal control was included, and no comparison could be conducted between blots. This drawback had been considered and internal control will be used in future experiment. The decrease in pPLN may occur through two mechanisms. First, PLN can be phosphorylated by PKA. Liu *et al* reported that the PKA level in ischaemia-induced MI was initially increased by 100-1000 fold due to elevated levels of catecholamine which activate the sympathetic nervous system (Liu *et al.*, 2021). Persistent ischaemia results in chronic stress and activation of β-AR. As a consequence, this desensitizes the β-AR via enhanced G-protein receptor kinase and β-arrestin signalling and induces remodelling changes that result in decreased surface expression of these receptors (Ruffolo and Kopia, 1986; Lohse, Engelhardt and Eschenhagen, 2003). In addition, the synthesis of cAMP and PKA activation are reduced. PKA can also induce homologous desensitization of β-AR by phosphorylating the receptor, which decreases the transmission of β-AR signals to affect PLN phosphorylation (Post et al., 1996, 1999).

Another putative protective mechanism initiated to counteract β-AR overstimulation is the upregulation of phosphodiesterases, a group of enzymes that hydrolyze cAMP, thereby decreasing potentially deleterious over-activation of PKA (Moorthy, Gao and Anand, 2011). Given the PKA is a major kinase that phosphorylated PLN, a reduction in PKA activity and level may results in a decrease pPLN level, as was the case

observed in the present study. Both cAMP and PKA are downstream effectors of β-AR signalling. There is evidence that the β_1 subtype expression is decreased by up to ≈50%, in heart failure while the expression of β_2-receptor remains unchanged in most studies (Ungerer *et al.*, 1993). Altogether, these results imply that the decrease in β-AR availability/downstream signalling and alterations to several effectors along the β-AR/cAMP/PKA pathway may explain the observed reduction in pPLN in the present MI model. However, these upstream factors were not investigated. Therefore, future studies should comprehensively analyse these factors to reveal the mechanism leading to the reduction in pPLN.

Apart from PKA-mediated phosphorylation of PLN, CAMKII phosphorylates PLN. This kinase also regulates other calcium-handling proteins including RyRs and the L-type channel (Grueter *et al.*, 2006; Uchinoumi *et al.*, 2016). Elevated expression of CaMKII is a common feature of heart failure development (Bossuyt *et al.*, 2008). Addition findings demonstrating the association of CaMKII with heart failure are those from animal model studies experiments demonstrating that pharmacological or genetic CaMKII inhibition prevents heart failure–related changes (i.e., dysfunction, hypertrophy, and arrhythmias) (Wu *et al.*, 2006). In some clinical studies and preclinical animal models of heart failure, it was demonstrated that CAMKII production was increased (Schulman and Anderson, 2010). Excessive CAMKII production can lead to SR Ca^{2+} overload and Ca^{2+} leak, both of which contribute to arrhythmogenesis (Anderson, Brown and Bers, 2011). CAMKII inhibition through gene therapy improved heart failure and restored the balance in the ECC process (Zhang *et al.*, 2005).

4.6 PP1 as HF therapeutical target

The PP1 dephosphorylates PLN thereby increasing its inhibitory activity on SERCA. It was found to be increased during heart failure (Neumann *et al.*, 1997; Sequeira and Maack, 2018). For instance, its expression in patients with end-stage heart failure was elevated (Huang *et al.*, 1999; El-Armouche *et al.*, 2004), and this was parallel with a reduction in pPLN. This suggests that strategies aimed at restoring PLN phosphorylation and inhibiting PP1 activity are potential therapeutic agents for the treatment of heart failure patients. Indeed, a recent study developed a decoy peptide mimicking phosphorylated PLN. This peptide increased pPLN levels and improved left ventricular developed pressure making it an ideal modality for restoring SERCA2a

activity in failing hearts (Oh *et al.*, 2013)**.** In view of these results, the decline in pPLN observed in this MI model may be hypothesised to arise through several routes. Our findings are congruent with prior reports that pPLN is reduced in failing hearts. Given that PKA and PP1 phosphorylate and dephosphorylates PLN, respectively, it will be interesting to simultaneously determine the levels and activity of these two opposing enzymes in the context of heart failure. We speculate that the decreased in pPLN in the present study may be due to increased PP1 activity and reduced CaMKII and PKA. Elucidation of this concept may provide the knowledge needed to develop drugs targeting SERCA and/or PLN for the management of heart failure patients.

5. Conclusion

This study found that protein expression of SERCA was increased in a sheep MI model while that of PLN remained unchanged. Interestingly, the protein level of pPLN was decreased, demonstrating that PLN is downregulated during the pathogenesis of heart failure. The results also showed that not all SERCA interacts with PLN, and PLN is likely to form pentamers under β-adrenergic phosphorylation. Going forward, addition investigations into the sub-cellular distribution of SERCA and PLN in normal and heart failure myocardium are advocated to reveal potential new therapeutic targets for combating heart failure.

6. Future perspectives

The non-significant decrease in pPLN expression in our MI model may be due to other unidentified factors. Therefore, we shall continue to measure the protein expression in MI sheep to determine whether this reduction in pPLN will become significant as the number of animals is increased, and pPLN/PLN ratio will be measured. Also, the sub-cellular distribution of SERCA and PLN will be further examined before and after isoprenaline treatment to clarify the present results and repeated in MI model when available. Concentration gradient of isoprenaline will also be added to reinforce the relationship between the distribution and catecholamine response. If redistribution is observed, the trafficking mechanism driving the rearrangement, e.g., the NEST pathway, will be studied. NCX upregulation had been found in compensation to the decrease

of SERCA, which would led to an accumulation of sodium intracellularly that worsen the heart failure situation.

Reference

Adachi, T. *et al.* (2004) 'S-glutathiolation by peroxynitrite activates SERCA during arterial relaxation by nitric oxide', *Nature Medicine*, 10(11), pp. 1200–1207. doi: 10.1038/nm1119.

Akin, B. L. *et al.* (2013) 'The structural basis for phospholamban inhibition of the calcium pump in sarcoplasmic reticulum', *Journal of Biological Chemistry*, 288(42), pp. 30181–30191. doi: 10.1074/JBC.M113.501585.

Alsafwah, S. *et al.* (2007) 'Congestive heart failure is a systemic illness: A role for minerals and micronutrients', *Clinical Medicine and Research*. Marshfield Clinic, pp. 238–243. doi: 10.3121/cmr.2007.737.

Anderson, M. E., Brown, J. H. and Bers, D. M. (2011) 'CaMKII in myocardial hypertrophy and heart failure', *Journal of Molecular and Cellular Cardiology*. J Mol Cell Cardiol, pp. 468–473. doi: 10.1016/j.yjmcc.2011.01.012.

Andersson, K. B. *et al.* (2009) 'Moderate heart dysfunction in mice with inducible cardiomyocyte-specific excision of the Serca2 gene', *Journal of Molecular and Cellular Cardiology*, 47(2), pp. 180–187. doi: 10.1016/j.yjmcc.2009.03.013.

Asahi, M. *et al.* (2000) 'Physical interactions between phospholamban and sarco(endo)plasmic reticulum Ca2+-ATPases are dissociated by elevated Ca2+, but not by phospholamban phosphorylation, vanadate, or thapsigargin, and are enhanced by ATP', *The Journal of biological chemistry*, 275(20), pp. 15034–15038. doi: 10.1074/JBC.275.20.15034.

Bathe-Peters, M. *et al.* (2021) 'Visualization of β-adrenergic receptor dynamics and differential localization in cardiomyocytes', *Proceedings of the National Academy of Sciences of the United States of America*, 118(23). doi: 10.1073/PNAS.2101119118.

Bers, D. M. (2000) 'Calcium fluxes involved in control of cardiac myocyte contraction', *Circulation Research*, pp. 275–281. doi: 10.1161/01.RES.87.4.275.

Bers, D. M. (2001) 'Excitation-Contraction Coupling and Cardiac Contractile Force', 237. doi: 10.1007/978-94-010-0658-3.

Bers, D. M. (2014) 'Cardiac sarcoplasmic reticulum calcium leak: Basis and roles in cardiac dysfunction', *Annual Review of Physiology*. Annual Reviews, pp. 107–127. doi: 10.1146/annurev-physiol-020911-153308.

Beuckelmann, D. J., Näbauer, M. and Erdmann, E. (1992) 'Intracellular calcium handling in isolated ventricular myocytes from patients with terminal heart failure', *Circulation*, 85(3), pp. 1046–1055. doi: 10.1161/01.CIR.85.3.1046.

Bhupathy, P., Babu, G. J. and Periasamy, M. (2007) 'SARCOLIPIN AND PHOSPHOLAMBAN AS REGULATORS OF CARDIAC SARCOPLASMIC RETICULUM CA2+ ATPASE', *Journal of molecular and cellular cardiology*, 42(5), p. 903. doi: 10.1016/J.YJMCC.2007.03.738.

De Boer, R. A. *et al.* (2001) 'Early expression of natriuretic peptides and SERCA in mild heart failure: Association with severity of the disease', *International Journal of Cardiology*, 78(1), pp. 5–12. doi: 10.1016/S0167-5273(00)00440-X.

Bögeholz, N. *et al.* (2015) 'Suppression of Early and Late Afterdepolarizations by Heterozygous Knockout of the Na+/Ca2+ Exchanger in a Murine Model', *Circulation: Arrhythmia and Electrophysiology*, 8(5), pp. 1210–1218. doi: 10.1161/CIRCEP.115.002927.

Bossuyt, J. *et al.* (2008) 'Ca2+/calmodulin-dependent protein kinase IIδ and protein kinase D overexpression reinforce the histone deacetylase 5 redistribution in heart failure', *Circulation Research*, 102(6), pp. 695–702. doi: 10.1161/CIRCRESAHA.107.169755.

Brette, F., Komukai, K. and Orchard, C. H. (2002) 'Validation of formamide as a detubulation agent in isolated rat cardiac cells', *American Journal of Physiology - Heart and Circulatory Physiology*, 283(4 52-4). doi: 10.1152/ajpheart.00347.2002.

Briston, S. J. *et al.* (2011) 'Impaired β-adrenergic responsiveness accentuates dysfunctional excitation-contraction coupling in an ovine model of tachypacing-induced heart failure', *Journal of Physiology*, 589(6), pp. 1367–1382. doi: 10.1113/jphysiol.2010.203984.

Brittsan, A. G. *et al.* (2000) 'Maximal inhibition of SERCA2 Ca2+ affinity by phospholamban in transgenic hearts overexpressing a non-phosphorylatable form of phospholamban', *Journal of Biological Chemistry*, 275(16), pp. 12129–12135. doi: 10.1074/jbc.275.16.12129.

Brodde, O. E. (1993) 'Beta-adrenoceptors in cardiac disease', *Pharmacology and Therapeutics*, pp. 405–430. doi: 10.1016/0163-7258(93)90030-H.

Camacho, P. *et al.* (2016) 'Large mammalian animal models of heart disease', *Journal of Cardiovascular Development and Disease*. Multidisciplinary Digital Publishing Institute (MDPI). doi: 10.3390/jcdd3040030.

Carl, S. L. *et al.* (1995) 'Immunolocalization of sarcolemmal dihydropyridine receptor and sarcoplasmic reticular triadin and ryanodine receptor in rabbit ventricle and atrium', *Journal of Cell Biology*, 129(3), pp. 673–682. doi: 10.1083/jcb.129.3.673.

Chaplin, S. (2019) 'Chronic heart failure in adults: diagnosis and management', *Prescriber*, 30(1), pp. 16–18. doi: 10.1002/psb.1730.

Chen-Izu, Y. *et al.* (2006) 'Three-dimensional distribution of ryanodine receptor clusters in cardiac myocytes', *Biophysical Journal*, 91(1), pp. 1–13. doi: 10.1529/BIOPHYSJ.105.077180/ATTACHMENT/125EF6C1-E8F2-4F65-8289-04DF1529DEA8/MMC4.AVI.

Cheng, H. and Lederer, W. J. (2008) 'Calcium sparks', *Physiological Reviews*. American Physiological Society, pp. 1491–1545. doi: 10.1152/physrev.00030.2007.

Cheng, H., Lederer, W. J. and Cannell, M. B. (1993) 'Calcium sparks: Elementary events underlying excitation-contraction coupling in heart muscle', *Science*, 262(5134), pp. 740–744. doi: 10.1126/science.8235594.

Chu, G. *et al.* (2000) 'A single site (Ser16) phosphorylation in phospholamban is sufficient in mediating its maximal cardiac responses to β-agonists', *Journal of Biological Chemistry*, 275(49), pp. 38938–38943. doi: 10.1074/jbc.M004079200.

Cohn, J. N. (1996) 'The Management of Chronic Heart Failure', *New England Journal of Medicine*, 335(7), pp. 490–498. doi: 10.1056/nejm199608153350707.

Currie, S. and Smith, G. L. (1999) 'Enhanced phosphorylation of phospholamban and downregulation of sarco/endoplasmic reticulum Ca2+ ATpase type 2 (SERCA 2) in cardiac sarcoplasmic reticulum from rabbits with heart failure', *Cardiovascular Research*, 41(1), pp. 135–146. doi: 10.1016/S0008-6363(98)00241-7/2/41-1-135-FIG6.GIF.

Cutler, M. J. *et al.* (2012) 'Targeted sarcoplasmic reticulum Ca2+ ATPase 2a gene delivery to restore electrical stability in the failing heart', *Circulation*, 126(17), pp. 2095–2104. doi: 10.1161/CIRCULATIONAHA.111.071480.

Dibb, K. M. *et al.* (2004) 'Mechanisms underlying enhanced cardiac excitation contraction coupling observed in the senescent sheep myocardium', *Journal of Molecular and Cellular Cardiology*, 37(6), pp. 1171–1181. doi: 10.1016/j.yjmcc.2004.09.005.

Dieterle, T. *et al.* (2005a) 'Gene transfer of a phospholamban-targeted antibody improves calcium handling and cardiac function in heart failure', *Cardiovascular Research*, 67(4), pp. 678–688. doi: 10.1016/j.cardiores.2005.04.029.

Dieterle, T. *et al.* (2005b) 'Gene transfer of a phospholamban-targeted antibody improves calcium handling and cardiac function in heart failure', *Cardiovascular Research*, 67(4), pp. 678–688. doi: 10.1016/J.CARDIORES.2005.04.029.

Dougherty, A. H. *et al.* (1984) 'Congestive heart failure with normal systolic function', *The American journal of cardiology*, 54(7), pp. 778–782. doi: 10.1016/S0002-9149(84)80207-6.

Edwards, A. G. *et al.* (2018) 'Calcium Signaling in Cardiomyocyte Models With Realistic Geometries', in *Cardiac Electrophysiology: From Cell to Bedside: Seventh Edition*. doi: 10.1016/B978-0-323-44733-1.00033-X.

Edwards, A. G. *et al.* (2021) 'Sarcoplasmic Reticulum Calcium Release Is Required for Arrhythmogenesis in the Mouse', *Frontiers in Physiology*, 12, p. 1747. doi: 10.3389/fphys.2021.744730.

Eisner, D. A. *et al.* (2010) 'How does CaMKIIδ phosphorylation of the cardiac ryanodine receptor contribute to inotropy?', *Proceedings of the National Academy of Sciences of the United States of America*. doi: 10.1073/pnas.1008809107.

Eisner, D., Caldwell, J. and Trafford, A. (2013) 'Sarcoplasmic reticulum Ca-ATPase and heart failure 20 years later', *Circulation Research*, 113(8), pp. 958–961. doi: 10.1161/CIRCRESAHA.113.302187.

El-Armouche, A. *et al.* (2004) 'Decreased protein and phosphorylation level of the protein phosphatase inhibitor-1 in failing human hearts', *Cardiovascular Research*, 61(1), pp. 87–93. doi: 10.1016/j.cardiores.2003.11.005.

Franzini-Armstrong, C., Protasi, F. and Ramesh, V. (1999) 'Shape, size, and distribution of Ca2+ release units and couplons in skeletal and cardiac muscles', *Biophysical Journal*, 77(3), pp. 1528–1539. doi: 10.1016/S0006-3495(99)77000-1.

Galice, S. *et al.* (2018) 'Size matters: Ryanodine receptor cluster size affects arrhythmogenic sarcoplasmic reticulum calcium release', *Journal of the American Heart Association*, 7(13). doi: 10.1161/JAHA.118.008724.

Gauthier, C. *et al.* (1998) 'The negative inotropic effect of β3-adrenoceptor stimulation is mediated by activation of a nitric oxide synthase pathway in human ventricle', *Journal of Clinical Investigation*, 102(7), pp. 1377–1384. doi: 10.1172/JCI2191.

Gheorghiade, M. and Bonow, R. O. (1998) 'Chronic heart failure in the United States: A manifestation of coronary artery disease', *Circulation*. Lippincott Williams & Wilkins, pp. 282–289. doi: 10.1161/01.CIR.97.3.282.

Glaves, J. P. *et al.* (2011) 'Phosphorylation and mutation of phospholamban alter physical interactions with the sarcoplasmic reticulum calcium pump', *Journal of Molecular Biology*, 405(3), pp. 707–723. doi: 10.1016/j.jmb.2010.11.014.

Greenberg, B. *et al.* (2016) 'Calcium upregulation by percutaneous administration of gene therapy in patients with cardiac disease (CUPID 2): A randomised, multinational, double-

blind, placebo-controlled, phase 2b trial', *The Lancet*, 387(10024), pp. 1178–1186. doi: 10.1016/S0140-6736(16)00082-9.

Greve, G. *et al.* (1985) 'Ultrastructural studies of intercalated disc separations in the rat heart during the calcium paradox', *Research in Experimental Medicine*, 185(3), pp. 195–206. doi: 10.1007/BF01852033.

Grueter, C. E. *et al.* (2006) 'L-Type Ca2+ Channel Facilitation Mediated by Phosphorylation of the β Subunit by CaMKII', *Molecular Cell*, 23(5), pp. 641–650. doi: 10.1016/j.molcel.2006.07.006.

Guo, T., Gillespie, D. and Fill, M. (2012) 'Ryanodine receptor current amplitude controls Ca2+ sparks in cardiac muscle.', *Circulation research*, 111(1), pp. 28–36. doi: 10.1161/CIRCRESAHA.112.265652.

Gustavsson, M. *et al.* (2013) 'Allosteric regulation of SERCA by phosphorylationmediated conformational shift of phospholamban', *Proceedings of the National Academy of Sciences of the United States of America*, 110(43), pp. 17338–17343. doi: 10.1073/PNAS.1303006110/SUPPL_FILE/SAPP.PDF.

Gwathmey, J. K. *et al.* (no date) *Abnormal Intracellular Calcium Handling in Myocardium From Patients With End-Stage Heart Failure*. Available at: http://ahajournals.org.

Hadipour-Lakmehsari, S. *et al.* (2019) 'Nanoscale reorganization of sarcoplasmic reticulum in pressure-overload cardiac hypertrophy visualized by dSTORM', *Scientific Reports*, 9(1), pp. 1–17. doi: 10.1038/s41598-019-44331-y.

Haghighi, K. *et al.* (2003) 'Human phospholamban null results in lethal dilated cardiomyopathy revealing a critical difference between mouse and human', *Journal of Clinical Investigation*, 111(6), pp. 869–876. doi: 10.1172/JCI17892.

Hasenfuss, G. *et al.* (1994) 'Relation between myocardial function and expression of sarcoplasmic reticulum Ca2+-ATPase in failing and nonfailing human myocardium', *Circulation Research*, 75(3), pp. 434–442. doi: 10.1161/01.RES.75.3.434.

Home | ARRIVE Guidelines (no date). Available at: https://arriveguidelines.org/ (Accessed: 27 June 2022).

Hou, Y. *et al.* (2015) 'Nanoscale analysis of ryanodine receptor clusters in dyadic couplings of rat cardiac myocytes', *Journal of Molecular and Cellular Cardiology*, 80, pp. 45–55. doi: 10.1016/j.yjmcc.2014.12.013.

Huang, B. *et al.* (1999) 'Diminished basal phosphorylation level of phospholamban in the postinfarction remodeled rat ventricle: Role of β-adrenergic pathway, G(i) protein, phosphodiesterase, and phosphatases', *Circulation Research*, 85(9), pp. 848–855. doi: 10.1161/01.RES.85.9.848.

Huang, X., Song, Z. and Qu, Z. (2018) 'Determinants of early afterdepolarization properties in ventricular myocyte models', *PLOS Computational Biology*, 14(11), p. e1006382. doi: 10.1371/JOURNAL.PCBI.1006382.

Hulot, J. S. *et al.* (2017) 'Effect of intracoronary administration of AAV1/SERCA2a on ventricular remodelling in patients with advanced systolic heart failure: results from the AGENT-HF randomized phase 2 trial', *European Journal of Heart Failure*, 19(11), pp. 1534–1541. doi: 10.1002/ejhf.826.

Isenberg, G. and Klockner, U. (1982) 'Calcium tolerant ventricular myocytes prepared by preincubation in a "KB medium"', *Pflügers Archiv European Journal of Physiology*, 395(1), pp. 6–18. doi: 10.1007/BF00584963.

Iwanaga, Y. *et al.* (2004) 'Chronic phospholamban inhibition prevents progressive cardiac dysfunction and pathological remodeling after infarction in rats', *The Journal of Clinical Investigation*, 113(5), pp. 727–736. doi: 10.1172/JCI18716.

Jaski, B. E. *et al.* (2009) 'Calcium Upregulation by Percutaneous Administration of Gene Therapy in Cardiac Disease (CUPID Trial), a First-in-Human Phase 1/2 Clinical Trial', *Journal of Cardiac Failure*, 15(3), pp. 171–181. doi: 10.1016/j.cardfail.2009.01.013.

Jessup, M. *et al.* (2011) 'Calcium upregulation by percutaneous administration of gene therapy in cardiac disease (CUPID): A phase 2 trial of intracoronary gene therapy of sarcoplasmic reticulum Ca2+-ATPase in patients with advanced heart failure', *Circulation*, 124(3), pp. 304–313. doi: 10.1161/CIRCULATIONAHA.111.022889.

Ji, Y. *et al.* (2000) 'Disruption of a single copy of the SERCA2 gene results in altered Ca2+ homeostasis and cardiomyocyte function', *Journal of Biological Chemistry*, 275(48), pp. 38073–38080. doi: 10.1074/jbc.M004804200.

Kimura, Y. *et al.* (1997) 'Phospholamban Inhibitory Function Is Activated by Depolymerization *', *Journal of Biological Chemistry*, 272(24), pp. 15061–15064. doi: 10.1074/JBC.272.24.15061.

Kistamás, K. *et al.* (2020) 'Calcium Handling Defects and Cardiac Arrhythmia Syndromes', *Frontiers in Pharmacology*, 11. doi: 10.3389/FPHAR.2020.00072.

Koh, X. *et al.* (2006) 'A 3D Monte Carlo analysis of the role of dyadic space geometry in spark generation', *Biophysical Journal*, 90(6), pp. 1999–2014. doi: 10.1529/biophysj.105.065466.

Kolstad, T. R. *et al.* (2018) 'Ryanodine receptor dispersion disrupts Ca 2+ release in failing cardiac myocytes', *eLife*, 7. doi: 10.7554/eLife.39427.

Koss, K. L., Grupp, I. L. and Kranias, E. G. (1997) 'The relative phospholamban and SERCA2 ratio: A critical determinant of myocardial contractility', *Basic Research in Cardiology*, 92(1 SUPPL.), pp. 17–24. doi: 10.1007/bf00794064.

Kuo, I. Y. and Ehrlich, B. E. (2015) 'Signaling in muscle contraction', *Cold Spring Harbor Perspectives in Biology*, 7(2). doi: 10.1101/cshperspect.a006023.

Lakatta, E. G. and Sollott, S. J. (2002) 'Perspectives on mammalian cardiovascular aging: Humans to molecules', in *Comparative Biochemistry and Physiology - A Molecular and Integrative Physiology*. Pergamon, pp. 699–721. doi: 10.1016/S1095-6433(02)00124-1.

Lederer, W. J. and Tsien, R. W. (1976) 'Transient inward current underlying arrhythmogenic effects of cardiotonic steroids in Purkinje fibres.', *The Journal of Physiology*, 263(2), pp. 73–100. doi: 10.1113/JPHYSIOL.1976.SP011622.

Li, L. *et al.* (1998) 'Cardiac myocyte calcium transport in phospholamban knockout mouse: Relaxation and endogenous CaMKII effects', *American Journal of Physiology - Heart and Circulatory Physiology*, 274(4 43-4). doi: 10.1152/ajpheart.1998.274.4.h1335.

Li, L. *et al.* (2012) 'Sodium accumulation in SERCA knockout-induced heart failure', *Biophysical Journal*, 102(9), pp. 2039–2048. doi: 10.1016/j.bpj.2012.03.045.

Lipskaia, L. *et al.* (2014) 'Expression of sarco (endo) plasmic reticulum calcium ATPase (SERCA) system in normal mouse cardiovascular tissues, heart failure and atherosclerosis', *Biochimica et Biophysica Acta (BBA) - Molecular Cell Research*, 1843(11), pp. 2705–2718. doi: 10.1016/J.BBAMCR.2014.08.002.

Liu, G. *et al.* (2018) 'Altered sarco(endo)plasmic reticulum calcium adenosine triphosphatase 2a content: Targets for heart failure therapy', *Diabetes and Vascular Disease Research*. SAGE PublicationsSage UK: London, England, pp. 322–335. doi: 10.1177/1479164118774313.

Liu, Y. *et al.* (2021) 'Physiological and pathological roles of protein kinase A in the heart', *Cardiovascular Research*. doi: 10.1093/cvr/cvab008.

Lohse, M. J., Engelhardt, S. and Eschenhagen, T. (2003) 'What Is the Role of β-Adrenergic Signaling in Heart Failure?', *Circulation Research*. Lippincott Williams & Wilkins, pp. 896–906. doi: 10.1161/01.RES.0000102042.83024.CA.

Luo, W. *et al.* (1994) 'Targeted ablation of the phospholamban gene is associated with markedly enhanced myocardial contractility and loss of β-agonist stimulation', *Circulation Research*, 75(3), pp. 401–409. doi: 10.1161/01.RES.75.3.401.

Luo, W. *et al.* (1998) 'Transgenic approaches to define the functional role of dual site phospholamban phosphorylation', *Journal of Biological Chemistry*, 273(8), pp. 4734–4739. doi: 10.1074/jbc.273.8.4734.

Lyon, A. R. *et al.* (2020) 'Investigation of the safety and feasibility of AAV1/SERCA2a gene transfer in patients with chronic heart failure supported with a left ventricular assist device – the SERCA-LVAD TRIAL', *Gene Therapy*, 27(12), pp. 579–590. doi: 10.1038/s41434-020-0171-7.

MacLennan, D. H. and Kranias, E. G. (2003a) 'Phospholamban: A crucial regulator of cardiac contractility', *Nature Reviews Molecular Cell Biology*, pp. 566–577. doi: 10.1038/nrm1151.

MacLennan, D. H. and Kranias, E. G. (2003b) 'Phospholamban: A crucial regulator of cardiac contractility', *Nature Reviews Molecular Cell Biology*. Nature Publishing Group, pp. 566–577. doi: 10.1038/nrm1151.

Macquaide, N. *et al.* (2015) 'Ryanodine receptor cluster fragmentation and redistribution in persistent atrial fibrillation enhance calcium release', *Cardiovascular Research*, 108(3), pp. 387–398. doi: 10.1093/CVR/CVV231.

Maier, T., Güell, M. and Serrano, L. (2009) 'Correlation of mRNA and protein in complex biological samples', *FEBS Letters*. No longer published by Elsevier, pp. 3966–3973. doi: 10.1016/j.febslet.2009.10.036.

Mariani, J. A. *et al.* (2011) 'Augmentation of left ventricular mechanics by recirculation-mediated AAV2/1SERCA2a gene delivery in experimental heart failure', *European Journal of Heart Failure*, 13(3), pp. 247–253. doi: 10.1093/eurjhf/hfq234.

Mattiazzi, A. *et al.* (2015) 'Ca2+ Sparks and Ca2+ waves are the subcellular events underlying Ca2+ overload during ischemia and reperfusion in perfused intact hearts', *Journal of Molecular and Cellular Cardiology*, 79, pp. 69–78. doi: 10.1016/j.yjmcc.2014.10.011.

McMurray, J. J. and Stewart, S. (2000) 'Epidemiology, aetiology, and prognosis of heart failure', *Heart*. BMJ Publishing Group Ltd and British Cardiovascular Society, pp. 596–602. doi: 10.1136/heart.83.5.596.

Mercadier, J.-J. *et al.* (no date) 'Rapid Publication Altered Sarcoplasmic Reticulum Ca2+-ATPase Gene Expression in the Human Ventricle during End-Stage Heart Failure gene expression * heart failure-human left ventricle-myosin heavy chain mRNA * sarcoplas-mic reticulum Ca2+-ATPase mRNA'.

Meyer, M. *et al.* (1995) 'Alterations of sarcoplasmic reticulum proteins in failing human dilated cardiomyopathy', *Circulation*, 92(4), pp. 778–784. doi: 10.1161/01.CIR.92.4.778.

Mishra, S. *et al.* (2002) 'Molecular mechanisms of reduced sarcoplasmic reticulum Ca2+ uptake in human failing left ventricular myocardium', *Journal of Heart and Lung Transplantation*, 21(3), pp. 366–373. doi: 10.1016/S1053-2498(01)00390-4.

Moorthy, B. S., Gao, Y. and Anand, G. S. (2011) 'Phosphodiesterases catalyze hydrolysis of cAMP-bound to regulatory subunit of protein kinase A and mediate signal termination', *Molecular and Cellular Proteomics*, 10(2). doi: 10.1074/mcp.M110.002295.

Morita, H., Seidman, J. and Seidman, C. E. (2005) 'Genetic causes of human heart failure', *Journal of Clinical Investigation*. American Society for Clinical Investigation, pp. 518–526. doi: 10.1172/JCI24351.

Nahidiazar, L. *et al.* (2016) 'Optimizing imaging conditions for demanding multi-color super resolution localization microscopy', *PLoS ONE*, 11(7). doi: 10.1371/journal.pone.0158884.

Napolitano, R. *et al.* (1992) 'Phosphorylation of phospholamban in the intact heart. A study on the physiological role of the Ca2+-calmodulin-dependent protein kinase system', *Journal of Molecular and Cellular Cardiology*, 24(4), pp. 387–396. doi: 10.1016/0022-2828(92)93193-N.

Neumann, J. *et al.* (1997) 'Increased expression of cardiac phosphatases in patients with end-stage heart failure', *Journal of Molecular and Cellular Cardiology*, 29(1), pp. 265–272. doi: 10.1006/jmcc.1996.0271.

Nikolaev, V. O. *et al.* (2010) 'β2-adrenergic receptor redistribution in heart failure changes cAMP compartmentation', *Science*, 327(5973), pp. 1653–1657. doi: 10.1126/science.1185988.

O'Connor, C. M. *et al.* (1999) 'Continuous intravenous dobutamine is associated with an increased risk of death in patients with advanced heart failure: Insights from the Flolan International Randomized Survival Trial (FIRST)', *American Heart Journal*, 138(1), pp. 78–86. doi: 10.1016/S0002-8703(99)70250-4.

Oh, J. G. *et al.* (2013) 'Decoy peptides targeted to protein phosphatase 1 inhibit dephosphorylation of phospholamban in cardiomyocytes', *Journal of Molecular and Cellular Cardiology*, 56(1), pp. 63–71. doi: 10.1016/j.yjmcc.2012.12.005.

Packer, M. *et al.* (2010) 'Effect of Oral Milrinone on Mortality in Severe Chronic Heart Failure', *http://dx.doi.org/10.1056/NEJM199111213252103*, 325(21), pp. 1468–1475. doi: 10.1056/NEJM199111213252103.

Page, E. (1978) 'Quantitative ultrastructural analysis in cardiac membrane physiology', *American Journal of Physiology - Cell Physiology*, 4(3). doi: 10.1152/ajpcell.1978.235.5.c147.

Part 2: The Who's Who of Super Resolution Microscopy - Single Molecule Localisation techniques - Bitesize Bio (no date). Available at: https://bitesizebio.com/21069/part-2-the-whos-who-of-super-resolution-microscopy-single-molecule-localisation-techniques/ (Accessed: 28 June 2022).

Peng, W. *et al.* (2016) 'Structural basis for the gating mechanism of the type 2 ryanodine receptor RyR2', *Science*, 354(6310). doi: 10.1126/science.aah5324.

Ponikowski, P. *et al.* (2016) '2016 ESC Guidelines for the diagnosis and treatment of acute and chronic heart failure: The Task Force for the diagnosis and treatment of acute and chronic heart failure of the European Society of Cardiology (ESC)Developed with the special contribution of the Heart Failure Association (HFA) of the ESC', *European heart journal*, 37(27), pp. 2129-2200m. doi: 10.1093/EURHEARTJ/EHW128.

Powell-Wiley, T. M. *et al.* (2021) 'Obesity and Cardiovascular Disease A Scientific Statement From the American Heart Association', *Circulation*. Lippincott Williams & Wilkins Hagerstown, MD, pp. E984–E1010. doi: 10.1161/CIR.0000000000000973.

Qaisar, R. *et al.* (2021) 'Restoration of Sarcoplasmic Reticulum Ca2+ ATPase (SERCA) Activity Prevents Age-Related Muscle Atrophy and Weakness in Mice', *International Journal of Molecular Sciences*, 22(1), pp. 1–14. doi: 10.3390/IJMS22010037.

Qin, F. *et al.* (2013) 'Hydrogen Peroxide–Mediated SERCA Cysteine 674 Oxidation Contributes to Impaired Cardiac Myocyte Relaxation in Senescent Mouse Heart', *Journal of the American Heart Association*, 2(4). doi: 10.1161/JAHA.113.000184.

Reuter, H. and Seitz, N. (1968) 'The dependence of calcium efflux from cardiac muscle on temperature and external ion composition', *The Journal of Physiology*, 195(2), pp. 451–470. doi: 10.1113/jphysiol.1968.sp008467.

Rodgers, J. L. *et al.* (2019) 'Cardiovascular risks associated with gender and aging', *Journal of Cardiovascular Development and Disease*. Multidisciplinary Digital Publishing Institute (MDPI). doi: 10.3390/jcdd6020019.

Ruffolo, R. R. and Kopia, G. A. (1986) 'Importance of receptor regulation in the pathophysiology and therapy of congestive heart failure', *The American Journal of Medicine*, 80(2 SUPPL. 2), pp. 67–72. doi: 10.1016/0002-9343(86)90148-8.

Santos, C. X. C. *et al.* (2011) 'Redox signaling in cardiac myocytes', *Free Radical Biology and Medicine*. Pergamon, pp. 777–793. doi: 10.1016/j.freeradbiomed.2011.01.003.

Sato, D. and Bers, D. M. (2011) 'How does stochastic ryanodine receptor-mediated Ca leak fail to initiate a Ca spark?', *Biophysical Journal*, 101(10), pp. 2370–2379. doi: 10.1016/J.BPJ.2011.10.017/ATTACHMENT/F8503546-025E-40A6-B968-5392D37866FB/MMC1.PDF.

Savarese, G. *et al.* (2021) 'Heart failure with mid-range or mildly reduced ejection fraction', *Nature Reviews Cardiology 2021 19:2*, 19(2), pp. 100–116. doi: 10.1038/s41569-021-00605-5.

Savarese, G. and Lund, L. H. (2017) 'Global Public Health Burden of Heart Failure', *Cardiac Failure Review*, 03(01), p. 7. doi: 10.15420/cfr.2016:25:2.

Sayadi, M. and Feig, M. (2013) 'Role of conformational sampling of Ser16 and Thr17-phosphorylated phospholamban in interactions with SERCA', *Biochimica et Biophysica Acta (BBA) - Biomembranes*, 1828(2), pp. 577–585. doi: 10.1016/J.BBAMEM.2012.08.017.

Schmidt, U. *et al.* (1999) 'Human heart failure: cAMP stimulation of SR Ca2+-ATPase activity and phosphorylation level of phospholamban', *American Journal of Physiology - Heart and Circulatory Physiology*, 277(2 46-2). doi: 10.1152/ajpheart.1999.277.2.h474.

Schulman, H. and Anderson, M. E. (2010) 'Ca2+/calmodulin-dependent protein kinase II in heart failure', *Drug Discovery Today: Disease Mechanisms*. Elsevier, pp. e117–e122. doi: 10.1016/j.ddmec.2010.07.005.

Schwinger, R. H. G. *et al.* (1995) 'Unchanged protein levels of SERCA II and phospholamban but reduced Ca2+ uptake and Ca2+-ATPase activity of cardiac sarcoplasmic reticulum from dilated cardiomyopathy patients compared with patients with nonfailing hearts', *Circulation*, 92(11), pp. 3220–3228. doi: 10.1161/01.CIR.92.11.3220.

Schwinger, R. H. G. *et al.* (1999) 'Reduced Ca2+-sensitivity of SERCA 2a in failing human myocardium due to reduced serin-16 phospholamban phoshorylation', *Journal of Molecular and Cellular Cardiology*, 31(3), pp. 479–491. doi: 10.1006/jmcc.1998.0897.

Sen, L. *et al.* (2000) 'Differences in mechanisms of SR dysfunction in ischemic vs. idiopathic dilated cardiomyopathy', *https://doi.org/10.1152/ajpheart.2000.279.2.H709*, 279(2 48-2). doi: 10.1152/AJPHEART.2000.279.2.H709.

Sequeira, V. and Maack, C. (2018) 'Rebalancing protein phosphorylation in heart failure to prevent arrhythmias', *European Journal of Heart Failure*. John Wiley & Sons, Ltd, pp. 1686–1689. doi: 10.1002/ejhf.1315.

Shacklock, P. S., Wier, W. G. and Balke, C. W. (1995) 'Local Ca2+ transients (Ca2+ sparks) originate at transverse tubules in rat heart cells.', *The Journal of Physiology*, 487(3), pp. 601–608. doi: 10.1113/jphysiol.1995.sp020903.

Sham, J. S. K., Jones, L. R. and Morad, M. (1991) 'Phospholamban mediates the β-adrenergic-enhanced Ca2+ uptake in mammalian ventricular myocytes', *American Journal of Physiology - Heart and Circulatory Physiology*, 261(4 30-4). doi: 10.1152/ajpheart.1991.261.4.h1344.

Shan, J. *et al.* (2010) 'Phosphorylation of the ryanodine receptor mediates the cardiac fight or flight response in mice', *Journal of Clinical Investigation*, 120(12), pp. 4388–4398. doi: 10.1172/JCI32726.

Shanmugam, M. *et al.* (2011) 'Ablation of phospholamban and sarcolipin results in cardiac hypertrophy and decreased cardiac contractility', *Cardiovascular Research*, 89(2), pp. 353–361. doi: 10.1093/cvr/cvq294.

Sikkel, M. B. *et al.* (2014) 'SERCA2a gene therapy in heart failure: an anti-arrhythmic positive inotrope', *British Journal of Pharmacology*, 171(1), pp. 38–54. doi: 10.1111/BPH.12472.

Simmerman, H. K. B. and Jones, L. R. (1998) 'Phospholamban: Protein structure, mechanism of action, and role in cardiac function', *Physiological Reviews*. American Physiological Society, pp. 921–947. doi: 10.1152/physrev.1998.78.4.921.

Solomon, S. D. *et al.* (2020) 'Sacubitril/Valsartan across the Spectrum of Ejection Fraction in Heart Failure', *Circulation*, 141(5), pp. 352–361. doi: 10.1161/CIRCULATIONAHA.119.044586.

Song, L. S. *et al.* (2006) 'Orphaned ryanodine receptors in the failing heart', *Proceedings of the National Academy of Sciences of the United States of America*, 103(11), pp. 4305–4310. doi: 10.1073/pnas.0509324103.

Song, Q. *et al.* (2003) 'Rescue of cardiomyocyte dysfunction by phospholamban ablation does not prevent ventricular failure in genetic hypertrophy', *The Journal of Clinical Investigation*, 111(6), pp. 859–867. doi: 10.1172/JCI16738.

Tada, M. *et al.* (1974) 'The Stimulation of Calcium Transport in Cardiac Sarcoplasmic Reticulum by Adenosine 3Ã¢â‚¬Â²:5Ã¢â‚¬Â²-Monophosphate-dependent Protein Kinase',

THE JOURNAL OF BIOLOGICAL CHEMIBTRY, 249(19), pp. 6174–6180. doi: 10.1016/S0021-9258(19)42237-0.

Tada, M., Kirchberger, M. A. and Katz, A. M. (1975) 'Phosphorylation of a 22,000-Dalton Component of the Cardiac Sarcoplasmic Reticulum by Adenosine 3' : S-Monophosphate-dependent Protein Kinase*', *Tam JOURNAL OF BIOLO~ICALCEE~~IIWRY*, 250(7), pp. 2640–2647. doi: 10.1016/S0021-9258(19)41650-5.

Tadini-Buoninsegni, F. *et al.* (2018) 'Drug interactions with the Ca2+-ATPase from Sarco(Endo)plasmic reticulum (SERCA)', *Frontiers in Molecular Biosciences*, 5(APR), p. 36. doi: 10.3389/FMOLB.2018.00036/BIBTEX.

Talukder, M. A. H. *et al.* (2008) 'Is reduced SERCA2a expression detrimental or beneficial to postischemic cardiac function and injury? Evidence from heterozygous SERCA2a knockout mice', *American Journal of Physiology - Heart and Circulatory Physiology*, 294(3). doi: 10.1152/ajpheart.01016.2007.

Taylor, C. J. *et al.* (2019) 'Trends in survival after a diagnosis of heart failure in the United Kingdom 2000-2017: population based cohort study', *The BMJ*, 364, p. 223. doi: 10.1136/bmj.l223.

Tokitsu, T. *et al.* (2016) 'Clinical Significance of Reactive Oxygen Species (ROS) in Heart Failure with Reduced Left Ventricular Ejection Fraction (HFrEF) Patients', *Journal of Cardiac Failure*, 22(9), p. S165. doi: 10.1016/j.cardfail.2016.07.074.

Toma, M. and Starling, R. C. (2010) 'Inotropic therapy for end-stage heart failure patients', *Current Treatment Options in Cardiovascular Medicine*, 12(5), pp. 409–419. doi: 10.1007/s11936-010-0090-9.

Toyoshima, C. *et al.* (2003) 'Modeling of the inhibitory interaction of phospholamban with the Ca2+ ATPase', *Proceedings of the National Academy of Sciences of the United States of America*, 100(2), pp. 467–472. doi: 10.1073/PNAS.0237326100.

Tunwell, R. E. A. *et al.* (1996) 'The human cardiac muscle ryanodine receptor-calcium release channel: identification, primary structure and topological analysis', *Biochemical Journal*, 318(2), pp. 477–487. doi: 10.1042/BJ3180477.

Uchinoumi, H. *et al.* (2016) 'CaMKII-dependent phosphorylation of RyR2 promotes targetable pathological RyR2 conformational shift', *Journal of Molecular and Cellular Cardiology*, 98, pp. 62–72. doi: 10.1016/j.yjmcc.2016.06.007.

Ungerer, M. *et al.* (1993) 'Altered expression of β-adrenergic receptor kinase and β1-adrenergic receptors in the failing human heart', *Circulation*, 87(2), pp. 454–463. doi: 10.1161/01.CIR.87.2.454.

Vafiadaki, E. *et al.* (2013) 'Identification of a protein phosphatase-1/phospholamban complex that is regulated by cAMP-dependent phosphorylation', *PLoS ONE*, 8(11). doi: 10.1371/journal.pone.0080867.

Valverde, C. A. *et al.* (2019) 'Ablation of phospholamban rescues reperfusion arrhythmias but exacerbates myocardium infarction in hearts with Ca2+/calmodulin kinase II constitutive phosphorylation of ryanodine receptors', *Cardiovascular Research*, 115(3), pp. 556–569. doi: 10.1093/CVR/CVY213.

Walden, A. P., Dibb, K. M. and Trafford, A. W. (2009) 'Differences in intracellular calcium homeostasis between atrial and ventricular myocytes', *Journal of Molecular and Cellular Cardiology*, 46(4), pp. 463–473. doi: 10.1016/j.yjmcc.2008.11.003.

Walker, M. A. *et al.* (2015) 'On the Adjacency Matrix of RyR2 Cluster Structures', *PLoS Computational Biology*, 11(11), p. e1004521. doi: 10.1371/journal.pcbi.1004521.

Watanabe, S. *et al.* (2017) 'Protein Phosphatase Inhibitor-1 Gene Therapy in a Swine Model of Nonischemic Heart Failure', *Journal of the American College of Cardiology*, 70(14), pp. 1744–1756. doi: 10.1016/J.JACC.2017.08.013.

Williams, G. S. B. *et al.* (2011) 'Dynamics of calcium sparks and calcium leak in the heart', *Biophysical Journal*, 101(6), pp. 1287–1296. doi: 10.1016/j.bpj.2011.07.021.

Wittmann, T., Lohse, M. J. and Schmitt, J. P. (2015) 'Phospholamban pentamers attenuate PKA-dependent phosphorylation of monomers', *Journal of Molecular and Cellular Cardiology*, 80, pp. 90–97. doi: 10.1016/j.yjmcc.2014.12.020.

Woo, A. Y. H. and Xiao, R. P. (2012) 'β-Adrenergic receptor subtype signaling in heart: From bench to bedside', *Acta Pharmacologica Sinica*. Nature Publishing Group, pp. 335–341. doi: 10.1038/aps.2011.201.

Wu, A. Z. *et al.* (2016) 'Phospholamban is concentrated in the nuclear envelope of cardiomyocytes and involved in perinuclear/nuclear calcium handling', *Journal of Molecular and Cellular Cardiology*, 100, pp. 1–8. doi: 10.1016/j.yjmcc.2016.09.008.

Wu, Y. *et al.* (2006) 'Suppression of dynamic Ca2+ transient responses to pacing in ventricular myocytes from mice with genetic calmodulin kinase II inhibition', *Journal of Molecular and Cellular Cardiology*, 40(2), pp. 213–223. doi: 10.1016/j.yjmcc.2005.11.005.

Xie, Y. *et al.* (2019) 'Size Matters: Ryanodine Receptor Cluster Size Heterogeneity Potentiates Calcium Waves', *Biophysical Journal*, 116(3), pp. 530–539. doi: 10.1016/j.bpj.2018.12.017.

Xu, J., Ma, H. and Liu, Y. (2017) 'Stochastic Optical Reconstruction Microscopy (STORM)', *Current protocols in cytometry*, 81, pp. 12.46.1-12.46.27. doi: 10.1002/CPCY.23.

Yancy, C. W. *et al.* (2013) '2013 ACCF/AHA guideline for the management of heart failure: Executive summary: A report of the American college of cardiology foundation/American Heart Association task force on practice guidelines', *Circulation*, 128(16), pp. 1810–1852. doi: 10.1161/CIR.0B013E31829E8807/-/DC2.

Zhang, M. and Shah, A. M. (2008) 'Reactive oxygen species in heart failure', in *Acute Heart Failure*, pp. 118–123. doi: 10.1007/978-1-84628-782-4_12.

Zhang, R. *et al.* (2005) 'Calmodulin kinase II inhibition protects against structural heart disease', *Nature Medicine*, 11(4), pp. 409–417. doi: 10.1038/nm1215.

Zima, A. V. *et al.* (2008) 'Termination of cardiac Ca2+ sparks: Role of intra-SR [Ca2+], release flux, and intra-SR Ca2+ diffusion', *Circulation Research*, 103(8), p. e105. doi: 10.1161/CIRCRESAHA.107.183236.

Zima, A. V. *et al.* (2010) 'Ca2+ spark-dependent and -independent sarcoplasmic reticulum Ca2+ leak in normal and failing rabbit ventricular myocytes', *The Journal of Physiology*, 588(23), pp. 4743–4757. doi: 10.1113/JPHYSIOL.2010.197913.

Zsebo, K. *et al.* (2014) 'Long-term effects of AAV1/SERCA2a gene transfer in patients with severe heart failure: Analysis of recurrent cardiovascular events and mortality', *Circulation Research*, 114(1), pp. 101–108. doi: 10.1161/CIRCRESAHA.113.302421.